Mucosal CD8+ T cell responses induced by an MCMV based vaccine vector confer protection against influenza challenge

Zheng, Xiaoyan; Oduro, Jennifer D.; Boehme, Julia D.; Borkner, Lisa; Ebensen, Thomas; Heise, Ulrike; Gereke, Marcus; Pils, Marina C.; Krmpotic, Astrid; Guzmán, Carlos A.; ...

Download date / Datum preuzimanja: **2025-03-10**

Repository / Repozitorij:

Repository of the University of Rijeka, Faculty of Medicine - FMRI Repository

RESEARCH ARTICLE

Mucosal CD8+ T cell responses induced by an MCMV based vaccine vector confer protection against influenza challenge

Xiaoyan Zheng[1], Jennifer D. Oduro[1], Julia D. Boehme[2,3], Lisa Borkner[1], Thomas Ebensen[1], Ulrike Heise[4], Marcus Gereke[2,3], Marina C. Pils[4], Astrid Krmpotic[5], Carlos A. Guzmán[1], Dunja Bruder[2,3], Luka Čičin-Šain[1,6]*

1 Department of Vaccinology and Applied Microbiology, Helmholtz Centre for Infection Research, Braunschweig, Germany, 2 Research Group Immune Regulation, Helmholtz Centre for Infection Research, Braunschweig, Germany, 3 Infection Immunology Group, Institute of Medical Microbiology, Infection Control and Prevention, Health Campus Immunology, Infectiology and Inflammation, Otto von-Guericke University, Magdeburg, Germany, 4 Mouse Pathology Unit, Helmholtz Centre for Infection Research, Braunschweig, Germany, 5 Department of Histology and Embryology, School of Medicine, University of Rijeka, Rijeka Croatia, 6 German Centre for Infection Research (DZIF), Partner site Hannover-Braunschweig, Germany

* luka.cicin-sain@helmholtz-hzi.de

Abstract

Cytomegalovirus (CMV) is a ubiquitous β-herpesvirus that establishes life-long latent infection in a high percentage of the population worldwide. CMV induces the strongest and most durable CD8$^+$ T cell response known in human clinical medicine. Due to its unique properties, the virus represents a promising candidate vaccine vector for the induction of persistent cellular immunity. To take advantage of this, we constructed a recombinant murine CMV (MCMV) expressing an MHC-I restricted epitope from influenza A virus (IAV) H1N1 within the immediate early 2 (*ie2*) gene. Only mice that were immunized intranasally (i.n.) were capable of controlling IAV infection, despite the greater potency of the intraperitoneally (i.p.) vaccination in inducing a systemic IAV-specific CD8$^+$ T cell response. The protective capacity of the i.n. immunization was associated with its ability to induce IAV-specific tissue-resident memory CD8$^+$ T (CD8T$_{RM}$) cells in the lungs. Our data demonstrate that the protective effect exerted by the i.n. immunization was critically mediated by antigen-specific CD8$^+$ T cells. CD8T$_{RM}$ cells promoted the induction of IFNγ and chemokines that facilitate the recruitment of antigen-specific CD8$^+$ T cells to the lungs. Overall, our results showed that locally applied MCMV vectors could induce mucosal immunity at sites of entry, providing superior immune protection against respiratory infections.

Author summary

Vaccines against influenza typically induce immune responses based on antibodies, small molecules that recognize the virus particles outside of cells and neutralize them before they infect a cell. However, influenza rapidly evolves, escaping immune recognition, and the fastest evolution is seen in the part of the virus that is recognized by antibodies.

Therefore, every year we are confronted with new flu strains that are not recognized by
our antibodies against the strains from previous years. The other branch of the immune
system is made of killer T cells, which recognize infected cells and target them for killing.
Influenza does not rapidly evolve to escape T cell killing; thus, vaccines inducing T-cell
responses to influenza might provide long-term protection. We introduced an antigen
from influenza into the murine cytomegalovirus (MCMV) and used it as a vaccine vector
inducing killer T-cell responses of unparalleled strength. Our vector controls influenza
replication and provides relief to infected mice, but only if we administered it through the
nose, to activate killer T cells that will persist in the lungs close to the airways. Therefore,
our data show that the subset of lung-resident killer T cells is sufficient to protect against
influenza.

Introduction

Respiratory infections caused by influenza viruses usually are associated with mild-to-moderate disease symptoms but are linked with high morbidity and mortality in susceptible populations like the elderly, young children, patients with co-morbidities and immunocompromised patients. Influenza virus causes seasonal epidemics, with typically 3 to 5 million cases of severe illness worldwide, according to WHO reports [1], and influenza type A viruses (IAV) cause the more severe disease form. Vaccines against influenza are based on the induction of adaptive immunity that targets the projected yearly epidemics. While most vaccines are based on inactivated IAV formulations inducing anti-IAV IgG responses, live attenuated influenza vaccines (LAIV) are also used as formulations for i.n. administration. This is based on the assumption that the induction of local immunity may provide superior immune protection [2, 3]. However, it remains unclear whether this protection depends on local IgA responses, on cytotoxic T cell responses, or on their combined antiviral activity. Of note, functional T cell responses were shown to substantially contribute to antiviral IAV immunity [4–6]. In particular, cytotoxic influenza-specific $CD8^+$ T lymphocytes (CTLs) promote viral clearance indirectly by secretion of pro-inflammatory cytokines such as IFNγ [7] and directly by perforin/Fas-mediated killing of infected epithelial cells in the bronchoalveolar space [8]. However, it remained unclear if T cell responses alone may control IAV, or if Ig responses were the crucial contributor to LAIV-mediated immune protection. We considered that this question could be addressed by developing a vaccine formulation that optimizes T cell responses against IAV while excluding the humoral ones.

CMV infection induces sustained functional T cell responses that are stronger in the long-term than the immune response to any other infectious pathogen [9]. Experiments in the mouse model have shown that defined CMV epitope-specific $CD8^+$ T cells accumulate in tissues and blood and are maintained at stable high levels during mouse CMV (MCMV) latency [10]. This phenomenon was termed "Memory Inflation" [11]. While some MCMV derived peptides, as the ones derived from the IE3 ($_{416}$RALEYKNL$_{423}$) and M139 proteins ($_{419}$TVYGFCLL$_{426}$) induce inflationary responses, other peptides, such as the M45-derived ($_{985}$HGIRNASFI$_{993}$), induce conventional $CD8^+$ T cell response [12]. Antigen-experienced $CD8^+$ T cells are subdivided into $CD62L^-$ effector memory ($CD8T_{EM}$) and $CD62L^+$ central memory $CD8^+$ T cells ($CD8T_{CM}$). The antigen-specific $CD8^+$ T cells during latent infection bear predominantly a $CD8T_{EM}$ phenotype and localize in secondary lymphoid or non-lymphoid organs [13]. They may provide immune protection against diverse viral targets [14–18], but also against bacterial [19] or tumor antigens [20, 21]. The exceptionally long-lasting

cellular immunity to CMV antigens has raised the interest in CMV as a potential new vaccine vector [14]. Many studies have demonstrated of optimal design of such CMV-based vaccines display efficient protection against virus infection such as rhesus macaque CMV (RhCMV) based Ebola [22] and SIV [23] vaccines and MCMV based Ebola virus vaccines [15]. *Erkes, D.A. and Qiu, Z.* et al. demonstrated that CMV based vaccine vectors provide protection in suppressing tumors [24, 25].

Both $CD8T_{EM}$ and $CD8T_{CM}$ subsets recirculate between the blood, the lymphoid organs, and the peripheral tissues. A special subset of memory $CD8^+$ T cells ($CD8T_{RM}$) resides in non-lymphoid tissues such as lungs, the female reproductive tract (FRT), the skin, the brain or the small intestine [26–29]. These cells lose the capacity of recirculating, maintain themselves at the site of infection, and their phenotype and transcriptional profile differ from classical memory T cells [30]. The well-characterized $CD8T_{RM}$ cells express C-type lectin CD69 [26] and the integrin $\alpha E \beta 7$, also known as CD103 [30]. They provide rapid and superior protection against pathogens at the site of infection [26, 30, 31]. A recent publication argued that a vaccine formulation adjuvanted by IL-1β enhances the immune control of IAV by improving mucosal T cell responses [32], but IL-1β improved both humoral and cellular responses in their study. Hence, the contribution of $CD8T_{RM}$ to IAV immune control remains unclear.

$CD8T_{RM}$ are found in the salivary glands of MCMV-infected animals [33], but not in their lungs [34]. We showed that i.n. infection with MCMV induces inflationary $CD8^+$ T cell responses, but also that memory inflation is more pronounced in relative and absolute terms upon i.p. infection [35]. The i.n. administration of an MCMV vaccine vector induced $CD8T_{RM}$ responses in the lungs [29] and only i.n. immunization restricted the replication of respiratory syncytial virus (RSV) upon challenge [29], indicating that $CD8T_{RM}$ elicited by i.n. administration of MCMV vectors might provide immune protection against respiratory virus infections, yet this evidence remains correlative. Upon antigen encounter, $CD8T_{RM}$ cells quickly reactivate at the mucosal site and secrete cytokines and chemokines or support the release of inflammatory mediators by other immune cells [28, 36, 37]. Lung airway $CD8T_{RM}$ cells provide protection against respiratory virus infection through IFNγ and help to recruit circulating memory $CD8^+$ T cells to the site of infection in an IFNγ-dependent way [36]. Therefore, to understand if $CD8T_{RM}$ cell may provide immune control of respiratory infections may help to refine strategies for tissue-targeted vaccine design.

In this study, we constructed an MCMV vector expressing the MHC-I restricted peptide $_{533}$**IYSTVASSL**$_{541}$ (**IVL**$_{533-541}$) [38] from IAV H1N1 hemagglutinin (HA)-MCMV^{IVL} under the transcriptional control of the *ie2* promotor. We investigated the potential of this recombinant virus to induce HA-specific $CD8^+$ T cells that confer protection against a lethal IAV challenge. We showed that i.n., but not i.p. immunization with MCMV^{IVL} resulted in robust protection against an IAV challenge. Protection following i.n. MCMV^{IVL} immunization was associated with high levels of antigen-specific $CD8T_{RM}$ cells in the lungs, and targeted depletion of lung-$CD8T_{RM}$ cells revealed that the control of the IAV in the lungs depended on these cells.

Results

Generation of recombinant MCMV and its replication *in vitro* and *in vivo*

We showed recently that MCMV vector expressing a single optimally positioned MHC-I restricted antigenic epitope provides a more efficient immune protection than vectors expressing the full-length protein [21]. Therefore, we constructed an MCMV influenza vaccine vector by inserting the coding sequence for the H-2K^d MHC-I restricted peptide **IYSTVASSL** from the hemagglutinin (HA) of the H1N1 (PR8) IAV [38] into the C-terminus of the MCMV *ie2* gene. The resulting recombinant virus was called MCMV^{IVL} (Fig 1A). To test if the
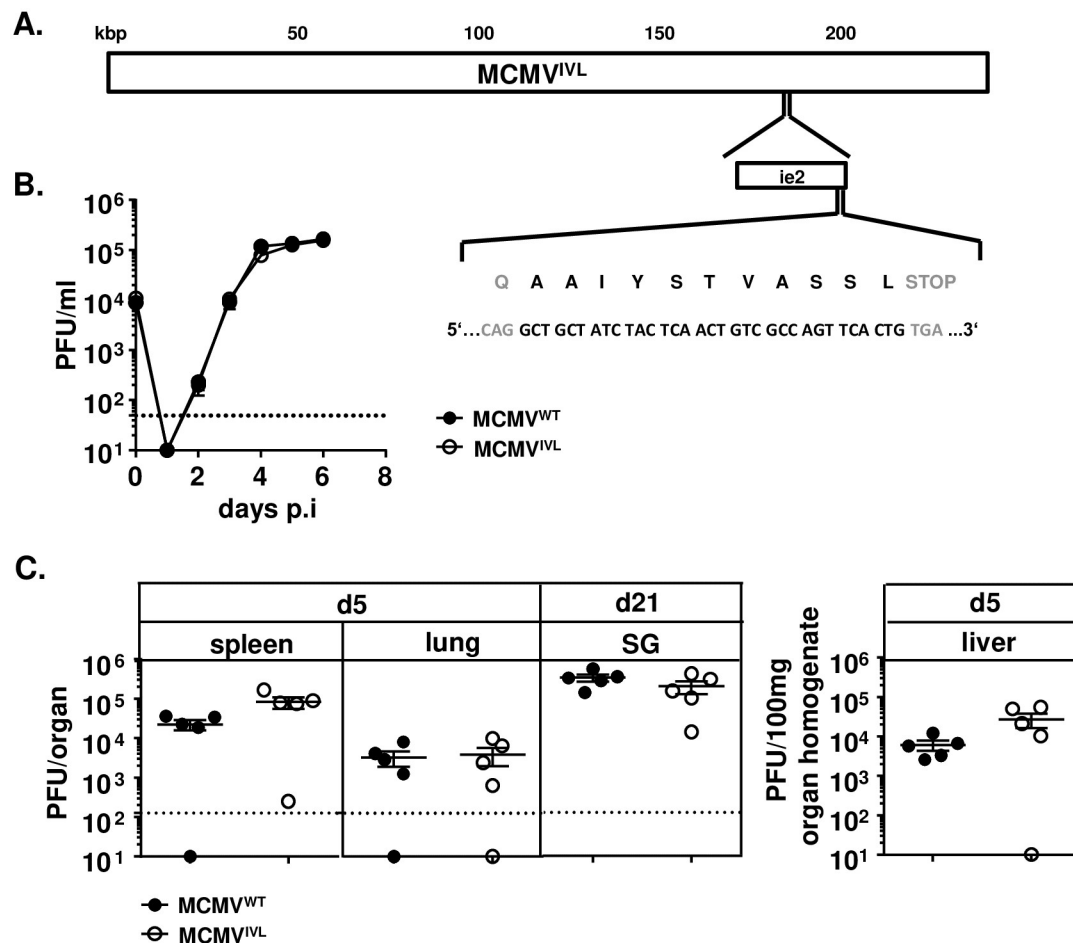
Fig 1. Generation of the recombinant MCMV expressing the $_{533}$IYSTVASSL$_{541}$ epitope. The sequence of IAV epitope $_{533}$AAIYSTVASSL$_{541}$ (IVL$_{533-541}$) was introduced at the C-terminus of the MCMV *ie2* gene, and the growth of the recombinant virus MCMV^{IVL} was tested *in vitro* and *in vivo*. (A) The location of the *ie2* gene within the MCMV genome at ~186-187kb position is shown; the insertion site of the peptide IVL$_{533-541}$ and the corresponding nucleotide sequences are magnified. (B) MCMV^{IVL} and wild-type MCMV (MCMV^{WT}) growth at a multiplicity of infection of 0.1 was compared in NIH-3T3 cells. Virus titers in supernatants expressed as plaque-forming units (PFU) were established at indicated time points. Group means +/- standard error of the mean (SEM) are shown. The dashed line indicates the limit of detection. (C) BALB/c mice were i.p. infected with 2 x 10^5 PFU of MCMV^{IVL} or MCMV^{WT} virus. Spleen, lung and liver homogenates were assayed for virus titers 5 days post-infection (dpi). Salivary-gland (SG) homogenates were assayed 21 dpi. Each symbol represents one mouse. Group means +/- standard error of the mean (SEM) are shown. The dashed line indicates the limit of detection.

https://doi.org/10.1371/journal.ppat.1008036.g001

recombinant virus retained its capacity to replicate in host cells, virus replication was assessed by multi-step growth kinetics assays in NIH-3T3 cells *in vitro* and by *ex vivo* quantification of virus titers in livers, lungs and spleens 5 days post-infection (dpi) and in salivary glands 21 dpi. MCMV^{IVL} showed identical replication properties as the MCMV^{WT}, both *in vitro* (Fig 1B) and *in vivo* (Fig 1C), indicating that the insertion of the IVL$_{533-541}$ epitope does not impair virus replication and spread.

Intranasal immunization with MCMV^{IVL} induces a lower magnitude of CD8$^+$ T cell response compared with intraperitoneal immunization

We have shown that mucosal infection with MCMV by the i.n. route induces memory inflation, although to a lower extent than upon the i.p. infection route [35]. To define if this pattern

would hold true for the artificially incorporated influenza epitope as well, we compared the magnitude of the CD8$^+$ T cell responses to MCMV^{IVL} and MCMV^{WT} induced via the i.n. and i.p. route, respectively. S1 Fig shows the gating strategy of flow cytometry analysis. The kinetics of antigen-specific CD8$^+$ T cell responses in peripheral blood was determined by IVL-tetramer staining. While we did not observe striking difference at early times post immunization, i.p. immunization induced an overall higher magnitude of inflationary CD8$^+$ T cell response during latency (Fig 2A and 2B). This pattern was observed both in relative terms (Fig 2A) and in absolute cell counts (Fig 2B). We next analyzed the IVL-specific CD8$^+$ T cell responses in spleens, lungs and mediastinal lymph nodes (mLNs) at times of latency (>3months post infection (p.i)). Similarly, i.p. immunization induced higher levels of IVL-specific CD8$^+$ T cells than the i.n. immunization in the spleen and lungs, both in relative (Fig 2C and 2D) and in absolute terms (Fig 2F and 2G). There were no significant differences in the mLNs (Fig 2E and 2H). In sum, mucosal (i.n.) immunization with MCMV^{IVL} induces a systemic inflationary IVL-specific CD8$^+$ T cell response, whereas the overall magnitude of the IAV-specific CD8$^+$ T cell response is less pronounced compared to that induced in i.p. immunized mice.

Intranasal immunization with MCMV^{IVL} facilitates the elimination of IAV is dependent on CD8$^+$ T cell

To test whether immunization with MCMV^{IVL} protects against IAV infection, latently immunized BALB/c mice were i.n. challenged with IAV. IAV titers in the lungs were quantified 5 dpi. Viral loads in mice that were immunized with MCMV^{WT} via either the i.p. or the i.n. route were comparable to those detected in mock-immunized mice (Fig 3A). In contrast, mice immunized with MCMV^{IVL} via the i.n. route showed significantly lower IAV titers than in any other group. Interestingly, i.p. MCMV^{IVL} immunization also resulted in reduced IAV loads, but to a lower extent than the i.n. immunization (Fig 3A). Similarly, animals immunized with MCMV^{WT} suffered the most severe weight loss whilst i.n. immunization of MCMV^{IVL} led to the least pronounced body weight loss. I.p. immunization with MCMV^{IVL} displayed an intermediate level (Fig 3B). Numerous studies have reported that CD8$^+$ T cells play an important role in protecting against influenza infection [39, 40] and it was reasonable to assume that our vector provided immune protection by eliciting CD8$^+$ T cell responses. To formally prove that efficient immune control of IAV observed in the MCMV^{IVL} (i.n.) immunized group depends on CD8$^+$ T cells, we depleted these cells by systemic treatment of mice with a depleting anti-CD8α antibody (depletion efficiency is shown in S2A Fig) one day prior to IAV challenge and quantified viral titers in lungs 6 dpi. While the virus titer was below the detection limit in mice that were i.n. immunized with MCMV^{IVL} and received isotype control antibodies, CD8$^+$ T cell depletion indeed resulted in a significant increase of the IAV titer to levels comparable to the groups that were i.p. immunized with MCMV^{IVL} and to control mice immunized with MCMV^{WT} by i.n. route (Fig 3C). CD8$^+$ T cell depletion also slightly increased virus titers in both control groups—MCMV^{IVL} (i.p.) and MCMV^{WT} (i.n.), but not as pronounced as in the MCMV^{IVL} i.n. immunized group (Fig 3C). Similar to Fig 3B, animals of all experimental groups showed a comparable body weight loss post-challenge, whereas i.n. MCMV^{IVL} immunized mice showed a faster recovery than the i.p. immunized mice (Fig 3D). Of note, this difference disappeared in the groups lacking CD8$^+$ T cells (Fig 3E). Together, these data demonstrate that IAV-specific CD8$^+$ T cells induced by the mucosal (i.n.) administration of MCMV^{IVL} confer protection against IAV in the lungs of vaccinated mice.

We further compared the lung pathology upon IAV challenge by histology. A moderate perivascular inflammation was observed in the lungs of most mice (stars) and to a lesser degree surrounding the bronchioles (arrows) (Fig 3F). The CD8$^+$ T cell depleted group showed more
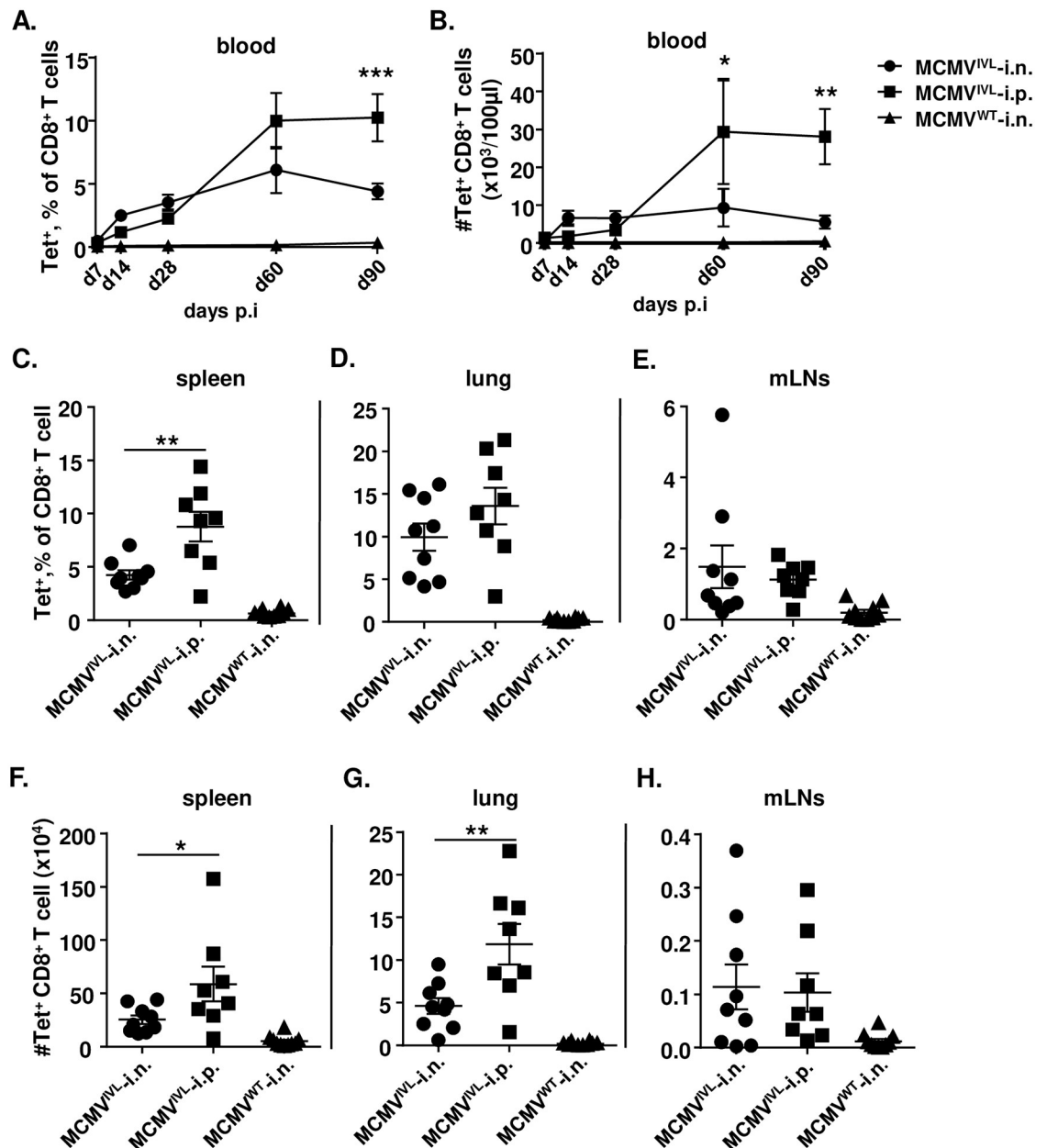
Fig 2. Intranasal immunization of MCMV[IVL] induces lower magnitude of CD8^{+} T cell response than intraperitoneal immunization. BALB/c mice were infected with 2×10^5 PFU MCMV[IVL] via the i.n. or i.p. route or with MCMV[WT] via the i.n. route. IVL-specific CD8^{+} T cell responses were analyzed by IVL-tetramers staining and flow cytometry. (A, B) Blood leukocytes were analyzed at indicated time points upon infection to define the (A) percentage of IVL-specific (Tet^{+}) cells among CD8^{+} T cells and (B) cell counts of IVL-specific (Tet^{+}) cells in peripheral blood. Two independent experiments were performed and results were pooled and shown as group means +/- SEM (n = 8–10). (E-H) IVL-specific CD8^{+} T cells in spleen, lungs and mLNs were quantified by IVL-tetramer staining 120 dpi as relative cell percentages among CD8^{+} T cells (C, D, E) or absolute cell counts (F, G, H) per organ. Two independent experiments were performed and pooled data are shown. Each symbol represents one mouse, n = 7–10. Group means +/- SEM are shown. Significance was assessed by Two-way ANOVA test (panels A, B) or one-way ANOVA test (Panels C-H). *P <0.05, **P<0.01, ***P<0.001.
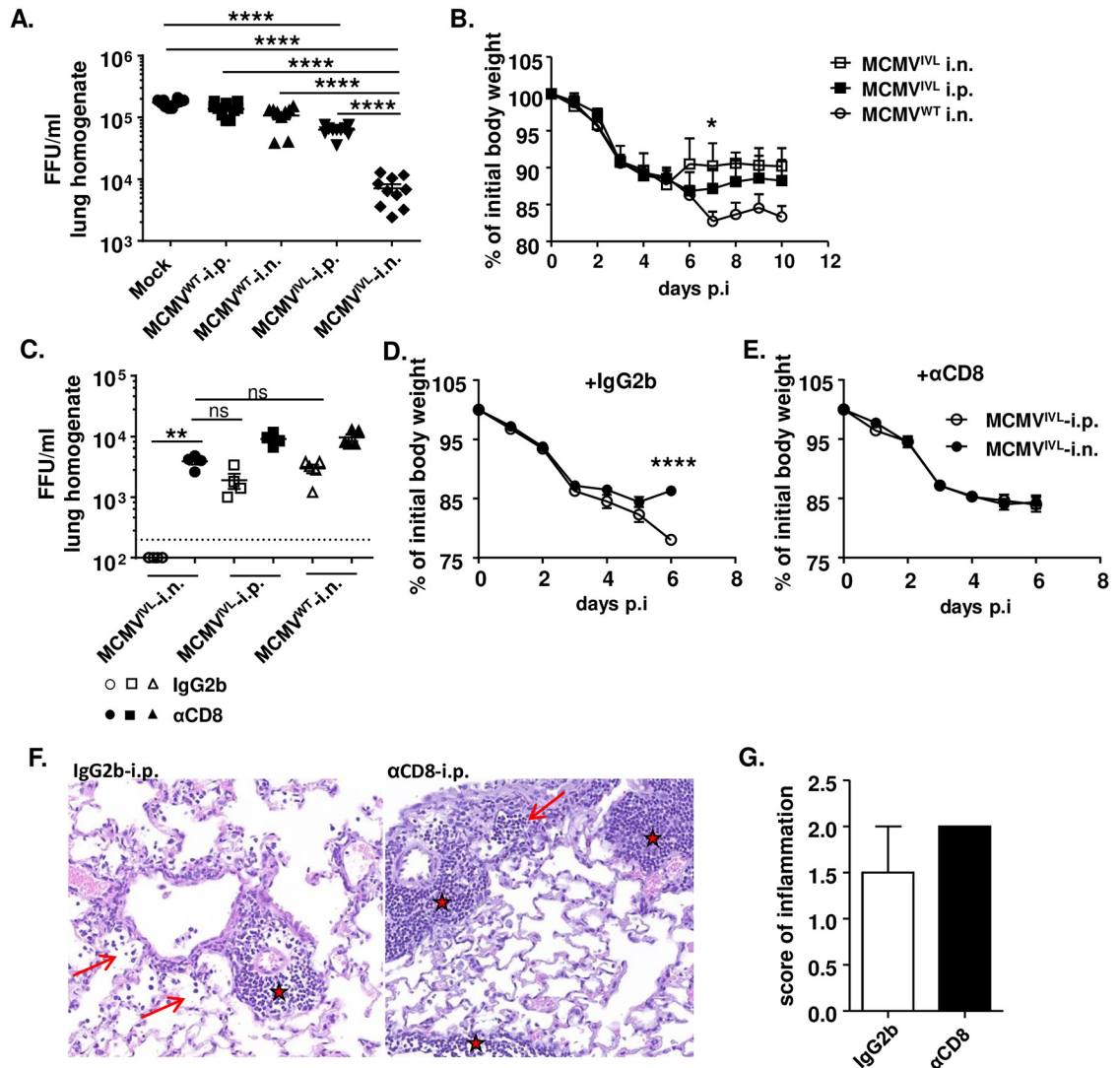
Fig 3. Intranasal immunization with MCMV^{IVL} facilitates the elimination of IAV. BALB/c mice were immunized with 2 x 10^5 PFU MCMV^{IVL} or MCMV^{WT} via the i.n. or i.p. route. Mock controls received 100 μl PBS by i.p. route. Once latency was established (> 3 months p.i), mice were challenged with IAV (PR8). (A) IAV titers in the lungs on day 5 post-challenge (i.n., 220 FFU) by focus-forming assay (FFA). Two independent experiments were performed and pooled data are shown, n = 10. (B) Body weight loss upon IAV challenge (i.n., 1100 FFU), n = 3–7. (C) CD8$^+$ T cells were depleted systemically by i.p. injection of 200 μg anti-CD8α antibody (αCD8) or isotype control antibody (IgG2b) one day before PR8 challenge (i.n., 1100 FFU). Virus loads in the lung homogenates were quantified on day 6 post-challenge by FFA. Two independent experiments were performed and one cohort was shown. Each symbol represents one mouse, n = 5. Group means +/- SEM are shown. (D, E) Body weight loss upon IAV challenge (i.n., 1100 FFU) without (D) or with (E) systemic CD8$^+$ T cell depletion. Two independent experiments were performed and pooled data are shown, n = 10. Group means +/-SEM are shown. (F) H&E staining of the lung tissue on day 5 post-challenge (i.n., 1100 FFU) with or without systemic depletion of CD8$^+$ T cell. (G) The score of inflammation in the lungs upon IAV challenge (i.n., 1100 FFU). Bars indicate means, error bars are SEM. Significance was assessed by One-way ANOVA test or Two-way ANOVA test. $^*P<0.05$, $^{**}P<0.01$, $^{****}P<0.0001$, ns: no significant difference.

severe pathology than isotype-treated controls, but the difference was not very pronounced (Fig 3G). Taken together, these data imply that intranasal immunization with the MCMV^{IVL} vector can limit IAV growth in the lungs by inducing IAV-specific CD8$^+$ T cell responses, whereas the clinical outcome is only moderately improved.

Intranasal immunization with MCMV^{IVL} induces antigen-specific tissue-resident memory CD8$^+$ T (CD8T$_{RM}$) cells in the lungs

We assumed that intranasal MCMV^{IVL} immunization may control the IAV replication by inducing CD8T$_{RM}$ cell responses in the lungs. In order to test this hypothesis, we identified the CD8T$_{RM}$ cell compartment by staining cells with the CD69 [26] and the CD103 [30] marker at times of MCMV latency ($>$ 3 months p.i.). It is known that resident memory T cells reside in the mucosal tissue layer and are non-migratory [31]. In this study, intravenous (i.v.) injection of a fluorescent anti-CD45 antibody prior sampling allows for the discrimination of circulating leukocytes (fluorescence-positive) from emigrated or tissue-resident leukocytes (fluorescence-negative). The CD69$^+$CD103$^+$ cells from lungs were virtually absent from the CD45-labelled fraction (Fig 4A). Barely CD8T$_{RM}$ could be detected in the spleen and blood regardless of the route of immunization (Fig 4B). CD8T$_{RM}$ (CD69$^+$CD103$^+$) cells were solely induced in the lungs and the frequency was significantly higher when i.n. immunized with MCMV^{IVL} than via the i.p. route (Fig 4B). Approximately forty percent of these lung CD8T$_{RM}$ cells were IVL-tetramer$^+$ which is significantly higher than the i.p. immunization group (Fig 4C). Similar results were observed when gated reversibly (Fig 4D) and when analyze these tetramer$^+$ CD8T$_{RM}$ cell numbers (Fig 4E). CD8T$_{RM}$ cells were also induced in the group that was i.n. immunized with MCMV^{WT}, but not IVL-specific (S3A Fig). In addition, there was an overall higher percentage of the CD69$^+$CD103$^-$CD8$^+$ T cells in the lungs of i.n. immunized mice (S3B Fig), although the absolute cell numbers did not show a significant difference (S3C Fig). Since CD69 and CD103 are imperfect markers of tissue residence, we validated if the CD69$^+$CD103$^+$ and CD69$^+$CD103$^-$ populations in lungs are truly CD8T$_{RM}$ by staining them for Eomesodermin (Eomes) expression, because CD8T$_{RM}$ cells show low expression of Eomes. Low levels of Eomes were observed in CD69$^+$CD103$^+$ CD8 T cells, whereas CD69$^+$CD103$^-$CD8$^+$ T cells showed high expression of Eomes which is consistent with primed CD8$^+$ T cells (S3D Fig). Hence the data suggested the CD69$^+$CD103$^-$ cell subset show distinct transcription profile from the CD8T$_{RM}$ cell. According to the expression of CD62L and KLRG1, IVL-specific CD8$^+$ T cells are classified into three subsets: effector (T$_{EFF}$: KLRG1$^+$CD62L$^-$); effector memory (T$_{EM}$: KLRG1$^-$CD62L$^-$) and central memory (T$_{CM}$: KLRG1$^-$CD62L$^+$) cells. The fractions of each subset in the mucosal (CD45$^-$) and circulation (CD45$^+$) in the blood, spleen and lung were analyzed (S4A & S4B Fig). While the fraction of CD8T$_{CM}$ cells remained relatively low in all compartments irrespectively of the route of administration, i.p. infection resulted in a response polarized towards T$_{EFF}$ cells, whereas i.n. immunization induced a larger fraction of T$_{EM}$ cells in all analyzed organs both in circulating and mucosal CD8$^+$ T cell subsets (S4A & S4B Fig). Majority of the IVL-specific CD8T$_{RM}$ cells show an EM phenotype (S4C Fig).

In summary, i.n. immunization with MCMV^{IVL} induces an accumulation of IAV-specific CD8T$_{RM}$ response in the lungs. Moreover, antigen-specific CD8$^+$ T cell responses induced via the mucosal route skew towards an effector memory phenotype.

Pulmonary CD8T$_{RM}$ cells improve viral clearance and the production of CD8$^+$ T cell-recruiting chemokines during IAV infection

Resident memory T cells reside in the epithelial barrier of mucosal tissue [31] that is in close proximity to the airways. Hence, they reactivate rapidly to a virus challenge at the site of infection upon encountering cognate antigens [29, 31]. To define the relevance of lung CD8T$_{RM}$ cells in protection against IAV challenge, we specifically depleted the airways CD8$^+$ T cells by i.n. administration of αCD8 antibodies one day before challenge (Fig 5A). Upon depletion, tetramer$^+$ CD8T$_{RM}$ cell number reduced significantly while the circulating CD8$^+$ T cell number did not change a lot in the lungs (S2B Fig). The local depletion did not affect the CD8$^+$ T cell
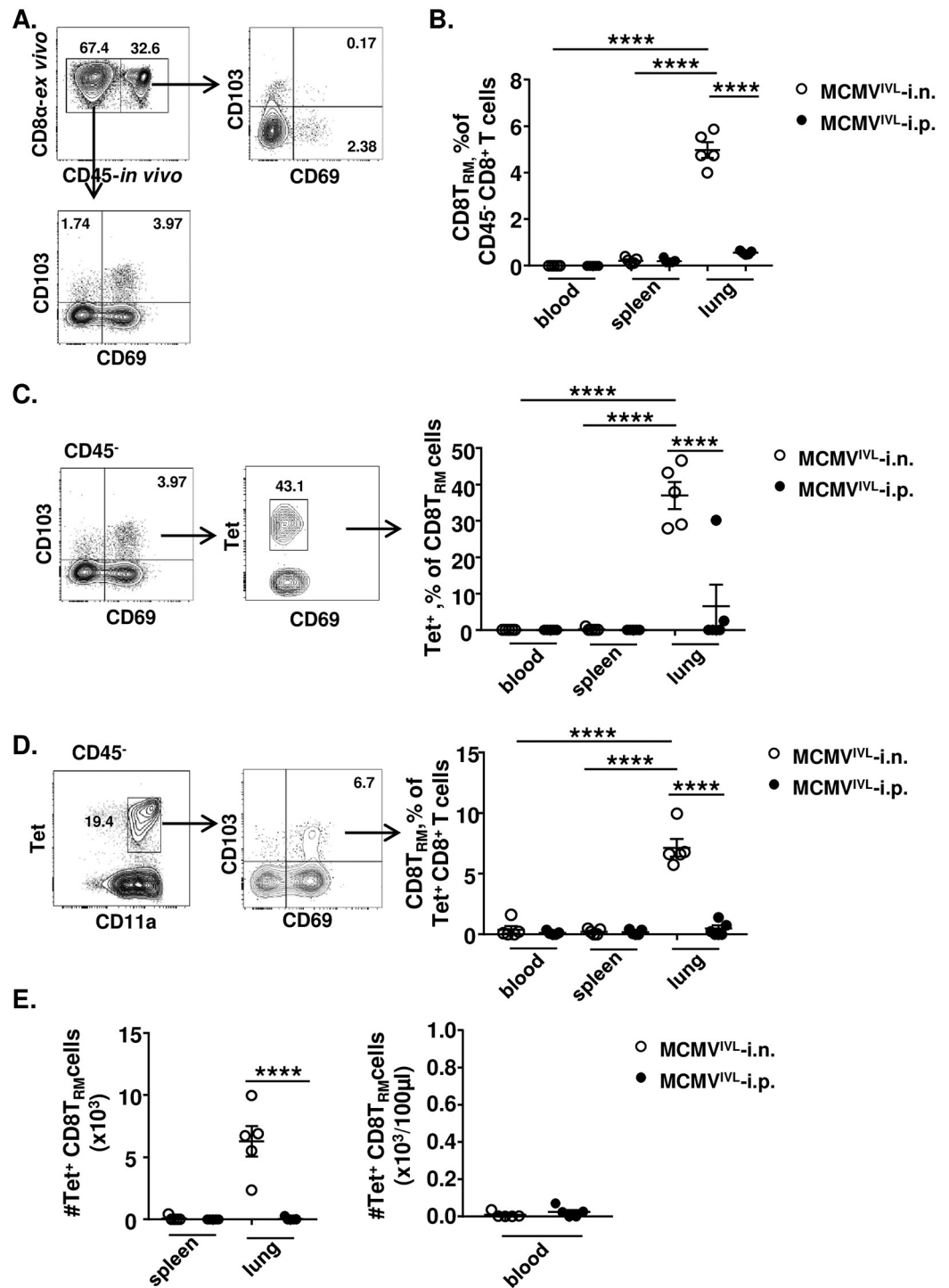
Fig 4. Intranasal immunization with the MCMV[IVL] induces antigen-specific tissue-resident CD8^{+} T cells in the lungs.
BALB/c mice were i.n. (○) or i.p. (●) infected with 2 x 10^{5} PFU of MCMV[IVL] virus. During latency (> 3 months p.i), anti-CD45 antibodies were injected intravenously 3–5 min before mice euthanasia. Leukocytes were isolated from peripheral blood, spleen and lungs, stained with antibodies against CD3, CD4, CD8α, CD11a, CD103, CD69, IVL-tetramer and measured by flow cytometry. (A) CD8T[RM] cells were gated as CD45^{-}CD69^{+}CD103^{+}. (B) Percentage of CD8T[RM] cells among CD45^{-} CD8^{+} T cells in the peripheral blood, spleen and lungs. (C) IVL-tetramer^{+} cells were gated on the CD8T[RM] cell subset and percentages of IVL-specific cells among CD8T[RM] cells in blood, spleen and lungs are shown. (D) CD8T[RM] cells were gated within the IVL-tetramer^{+} cell subset and the percentages of CD8T[RM] cells among tetramer^{+} CD8^{+} T cells in blood, spleen and lungs are shown. (E) The number of lung CD8T[RM] cells in spleen, lungs and blood of different groups. Two independent experiments were performed and pooled data are shown. Each symbol represents one mouse, n = 5. Group means +/- SEM are shown. Significance was assessed by One-way ANOVA. [**]P<0.01, [****]P<0.0001.
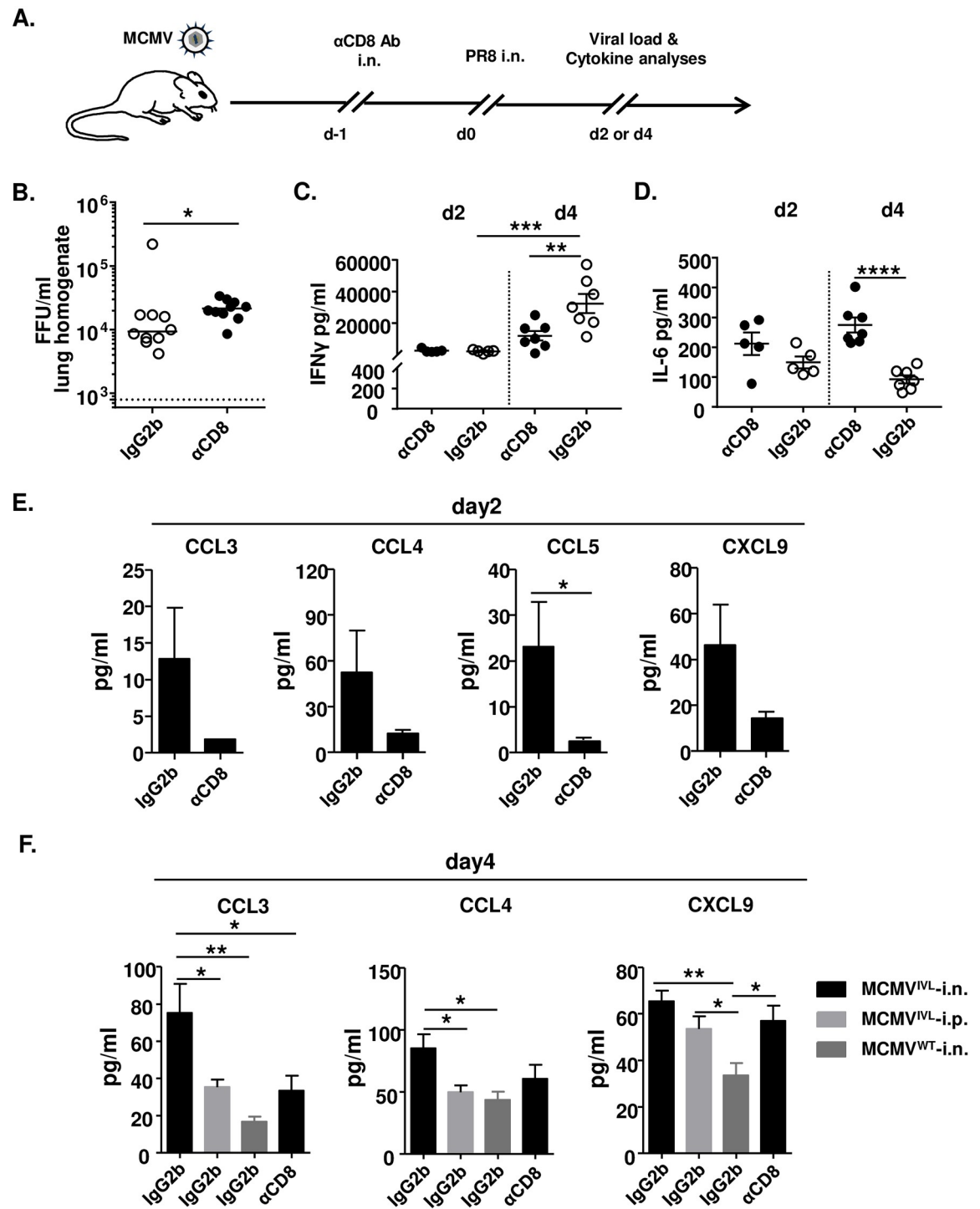
Fig 5. CD8T_{RM} cells facilitate the elimination of IAV. BALB/c mice were i.n. or i.p. immunized with 2 x 10⁵ PFU MCMV^IVL or i.n. with MCMV^WT. During latency (> 3 months p.i), mice were treated with αCD8 or IgG2b antibodies and challenged with IAV (PR8) (i. n., 1100 FFU). Leukocytes were isolated from lungs on day 4 post-challenge for flow cytometric analysis. (A) Graphic representation of the mucosal CD8⁺ T cell depletion protocol. (B) IAV titers in the lungs on day 4 post-challenge of MCMV^IVL i.n. immunized mice. Two independent experiments were performed and pooled data are shown. Each symbol represents one mouse, n = 10. Group medians are shown. (C-F) The concentration of inflammatory cytokines and chemokines were measured in the BALF on day 2 and day 4 post-IAV challenge. (C) The concentrations of IFNγ and (D) IL-6 in the BALF of each MCMV^IVL i.n. immunized mice are shown as symbols. Group means +/- SEM are shown. (E) The concentration of CCL3, CCL4, CCL5 and CXCL9 in the BALF on day 2 post-challenge. (F) The concentration of CCL3, CCL4 and CXCL9 in the BALF on day 4 post-challenge. Two independent experiments were performed and pooled data are shown. n = 5–7. Bars indicate means, error bars are SEM. Significance was assessed by Mann-Whitney U test, One-way ANOVA test, or Two-way ANOVA test. *P<0.05, **P<0.01, ***P<0.001, ****P<0.0001.

counts in the blood (S2C Fig). An earlier day was chosen (4 days post-challenge) to assess whether CD8T$_{RM}$ cell could rapidly confer protection. The IAV titers in the lungs of i.n. MCMV^{IVL} immunized mice were quantified. Targeted depletion of pulmonary CD8T$_{RM}$ cells was associated with a significantly higher viral burden during IAV infection (Fig 5B). These data indicate that CD8T$_{RM}$ cells induced by i.n. immunization with MCMV^{IVL} promote the clearance of IAV.

Influenza virus infection can induce a vigorous cytokine storm in airways and lungs, which promotes the recruitment of inflammatory cell. IFNγ as a pivotal antiviral cytokine is expressed early after influenza virus infection [41]. It has been demonstrated that CD8T$_{RM}$ cells activate rapidly when they re-encounter the cognate antigen and provide protection by secreting cytokines such as IFNγ and granzyme B [42, 43]. *Morabito et al.* showed that intranasal immunization with an MCMV-based vaccine vector induced CD8T$_{RM}$ cells and IFNγ was secreted at the very early time upon challenge during RSV infection [29].

Therefore, we measured the production of IFNγ in the bronchoalveolar lavage fluid (BALF) early upon challenge. IFNγ levels were generally low on day 2 post-challenge and no difference could be observed between groups regardless of airway CD8$^+$ T cells depletion (Fig 5C). On day 4, the IFNγ level was significantly increased compared to the level on day 2, but more IFNγ was induced in the control group than in the one lacking CD8T$_{RM}$ cell in the lungs (Fig 5C). IFNγ was also induced in the MCMV^{IVL} i.p. immunization group and extremely low level of IFNγ could be detected in the MCMV^{WT} control group (S5A Fig). These data suggest that primary cognate antigen immunization is needed for the rapid IFNγ secretion and that resident CD8$^+$ T cells may not be the major IFNγ producer. In contrast to these effects, depletion of lung airway CD8$^+$ T cells increased the concentration of IL-6 as compared to the group that was intranasally immunized with MCMV^{IVL} and treated with isotype control antibodies (Fig 5D). Similarly, a higher concentration of IL-6 was also detected in the i.p. immunization group, whereas the MCMV^{WT} control group displayed the highest IL-6 levels (S5B Fig). Very low levels of other cytokines could be detected in all groups, both on day 2 and 4 post-challenge and regardless of the depletion of the airway CD8$^+$ T cell (S5C Fig), suggesting that the presence of pulmonary CD8T$_{RM}$ cells does not affect the Th1, Th2 and Th17 immune profile during early IAV infection.

It has been demonstrated that T$_{RM}$ cells help to recruit immune cells to the infection site through the induction of chemokines such as CCL3 and CXCL9 in the female reproductive tract (FRT), and CCL4 in the lungs, either by direct chemokine expression or by their induction in nearby cells, such as epithelial cells [28, 29].

To determine whether i.n. immunization with MCMV^{IVL} induced inflammatory chemokines expression upon IAV challenge, a series of inflammatory chemokines were measured in the BALF on day 2 (Fig 5E) and day 4 (Fig 5F) upon IAV challenge. Airway depletion of CD8$^+$ T cells reduced CCL3, CCL4, CCL5 levels on day 2. On day 4, CCL3 and CCL4 levels were significantly higher in the MCMV^{IVL} i.n. group than in the MCMV^{IVL} i.p. and in the MCMV^{WT} i.n. immunization groups. Airway CD8$^+$ T cell depletion reduced the level of CCL3 and CCL4 to values in the i.p. MCMV^{IVL} immunization group (Fig 5F). CXCL9 levels were comparable between the MCMV^{IVL} i.n. and i.p. immunization groups, but dramatically lower in the MCMV^{WT} immunization group (Fig 5F), which was consistent with the low IFNγ level in the BALF, as IFNγ is known as an inducer of CXCL9, which then acts as a T cell-attracting chemokine. Together, these data indicate that CD8T$_{RM}$ cells induced by i.n. immunization with MCMV^{IVL} promote the induction of the pro-inflammatory chemokines CCL3, CCL4, CCL5 and CXCL9, along with a reduction of IL-6 in the lungs.

CD8T$_{RM}$ cells facilitate the expansion of CD8$^+$ T cells in the lungs

Since i.n. immunization induced stronger chemokine responses in comparison to the i.p. immunization route, we decided to define whether CD8T$_{RM}$ cells induced by MCMV^{IVL} promoted the accumulation of CD8$^+$ T cells in the lungs. We first analyzed the total IVL-specific and CD8$^+$ T cell numbers (CD45$^+$ plus CD45$^-$) in the MCMV^{IVL} i.n. immunization group. IVL-specific and CD8$^+$ T cell numbers increased from day 2 to day 4 post-challenge, but only in mice that were not depleted for airway CD8$^+$ T cells (Fig 6A and 6B). Both IVL-specific and total CD8$^+$ T cell counts increased significantly in the BALF of i.n. immunized mice by day 4 post IAV challenge (Fig 6C and 6D), However, in the mice which CD8$^+$ T cells were depleted prior to challenge, very few IVL-tetramer$^+$ CD8$^+$ T cells (Fig 6C, filled dots) and CD8$^+$ T cells (Fig 6D, filled dots) could be detected in the BALF, both on day 2 and at day 4 post-challenge. These data indicate that CD8$^+$ T cells accumulate in the lungs and migrate to the lung tissue and bronchoalveolar space upon IAV challenge. In addition, IVL-specific CD8$^+$ T cell counts in the lung tissue and BAL were slightly higher in the MCMV^{IVL} i.n. group than in the i.p. immunized group (S6A and S6B Fig). This differs from results prior to IAV challenge, where significantly larger amounts of IVL-specific CD8$^+$ T cells were detected in the i.p. group (Fig 2G).

CD8$^+$ T cells in the lung tissue were further analyzed by *in vivo* labeling with anti-CD45 antibodies in the presence or absence of airway CD8$^+$ T cells. The IVL-specific CD8$^+$ T cell population failed to expand upon airway CD8$^+$ T cell depletion, with significantly lower numbers in CD45$^-$ subset on day 4. However, IAV-specific CD8$^+$ T cell counts showed an increasing trend both in the CD45$^+$ and in the CD45$^-$ subsets on day 4 post-challenge (Fig 6E). Airway CD8$^+$ T cell depletion prevented also the expansion of total CD8$^+$ T cells counts on day 4 (Fig 6F). Interestingly, in contrast to IVL-specific CD8$^+$ T cells, only the CD45$^-$ fraction of the total CD8 pool expanded on day 4 (Fig 6F), suggesting that bystander CD8$^+$ T cells were also accumulated within the lungs. The depletion effects were more pronounced later upon antibody administration. Hence, direct depletion of incoming cells appears an unlikely scenario. Together with the increased chemokines in the BAL, these data indicate that the increase of IVL-specific CD8$^+$ T cells upon challenge is not due to *in situ* proliferation or differentiation but most probably by recruiting CD8$^+$ T cells from circulating system.

We also checked whether CD8T$_{RM}$ cells expanded upon IAV challenge that may contribute to the accumulation of CD8$^+$ T cells. We found that the number of CD8T$_{RM}$ cells in the lungs did not expand from day 2 to day 4; if anything, their frequency decreased (Fig 7A and 7B). Likewise, IVL-Tetramer$^+$ CD8T$_{RM}$ cell counts were also slightly reduced from day 2 to day 4 post-challenge (Fig 7C), although IVL-Tetramer$^+$ CD8$^+$ T cell counts increased at the same time (Fig 6A). It seems that the effect of the i.n. depletion was local, since the frequencies (S6C and S6D Fig) and counts (S6E and S6F Fig) of IVL-specific CD8$^+$ T cells in the blood and spleen did not significantly differ upon αCD8 or isotype-control antibody i.n. administration. In addition, CD4$^+$ T cell numbers showed no difference upon IAV challenge when airway CD8$^+$ T cells were depleted compared with the control group (S7 Fig), suggesting that CD8T$_{RM}$ cell do not promote CD4$^+$ T cells trafficking into the lungs. Therefore, our data indicated that CD8T$_{RM}$ cells confer protection by recruiting circulating CD8$^+$ T cells upon IAV challenge.

Discussion

Influenza-specific CD8$^+$ T cells are known to contribute to virus elimination, as the clearance of influenza virus is delayed in T cell-deficient mice [5, 44]. However, previous evidence did not clarify whether vaccines solely inducing influenza-specific CD8$^+$ T cell responses improve
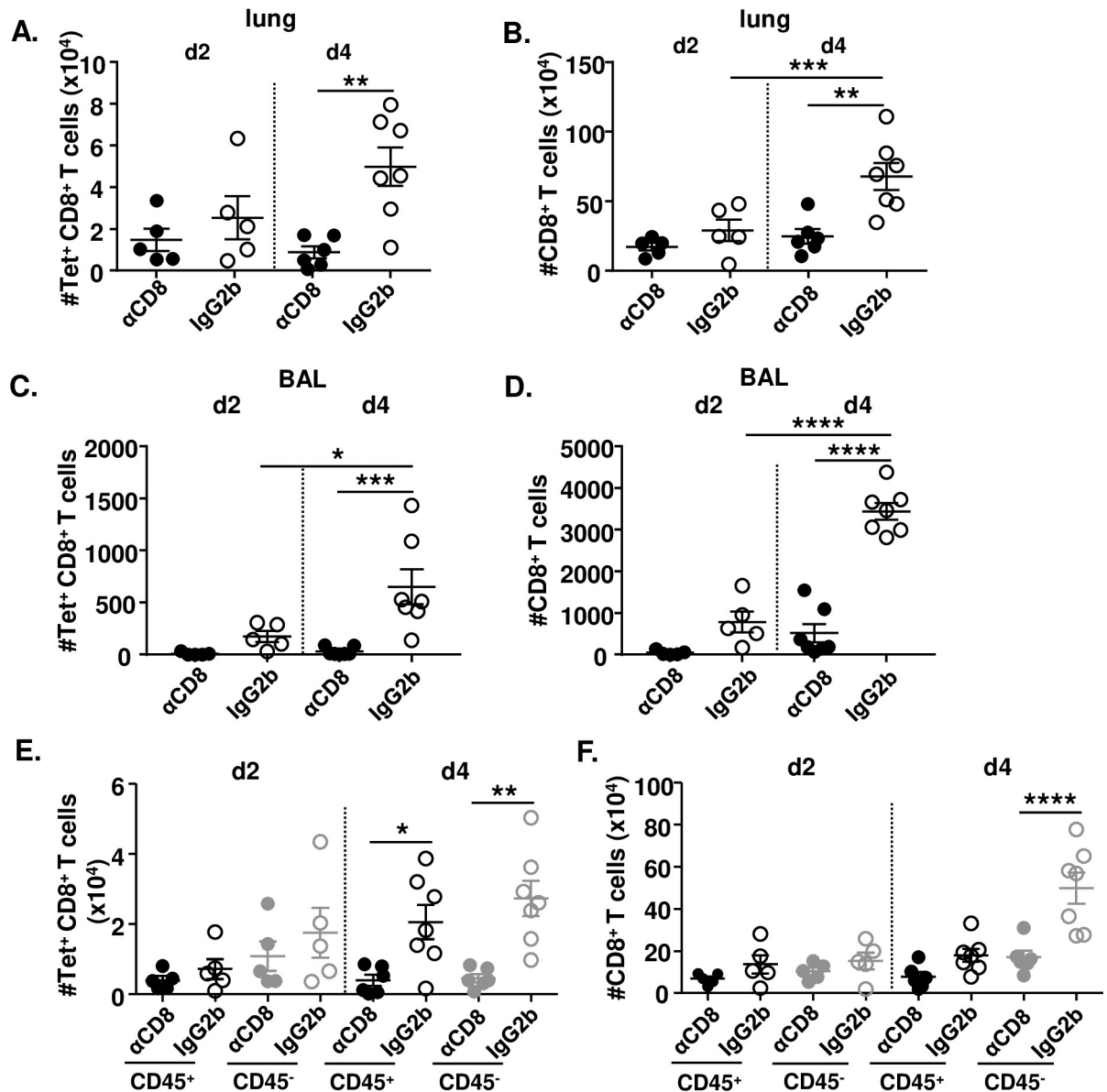
Fig 6. CD8T$_{RM}$ cells facilitate the accumulation of CD8$^+$ T cells in the lungs. BALB/c mice were immunized with 2 x 10^5 PFU MCMV^{IVL} via the i.n. route. During latency ($>$ 3 months p.i), mice were i.n. treated with αCD8 (black circle;grey circle) or IgG2b (black-lined circle; grey-lined circle) antibodies and challenged with IAV (PR8) (i.n., 1100 FFU) one day after. Anti-CD45 antibodies were injected intravenously 3–5 min before euthanasia. Leukocytes were isolated from lung tissue to analyze the CD8$^+$ T cell response on day 2 and day 4 post-challenge. (A) Total cell counts of IVL-specific CD8$^+$ T cells of both intravitally labeled (CD45$^+$) or unlabeled (CD45$^-$) in the lung tissue. (B) Total cell counts of CD8$^+$ T cells of both CD45$^+$ and CD45$^-$ in the lung tissue. (C) Cell counts of IVL-specific CD8$^+$ T cells in the BAL. (D) Cell counts of total CD8$^+$ T cells in the BAL. (E) IVL-specific CD8$^+$ T cells or (F) Total CD8$^+$ T cells that were intravitally labeled or remained unlabeled in the lung tissue were counted on day 2 or day 4 post IAV challenge. Two independent experiments were performed and pooled data are shown. Each symbol represents one mouse, n = 5–7. Group means +/- SEM are shown. Significance was assessed by One-way ANOVA test. *P $<$0.05, **P $<$0.01, ***P $<$0.001, ****P $<$0.0001.

https://doi.org/10.1371/journal.ppat.1008036.g006

immune protection. To avoid confounding humoral immune responses and focus on the potential of optimally primed CD8$^+$ T cells in protecting against influenza, we generated a new MCMV based vaccine vector. CMV vaccine vectors expressing exogenous antigenic peptides fused to a CMV gene induce CD8$^+$ T cell responses of unparalleled strength [14, 15, 21, 29].
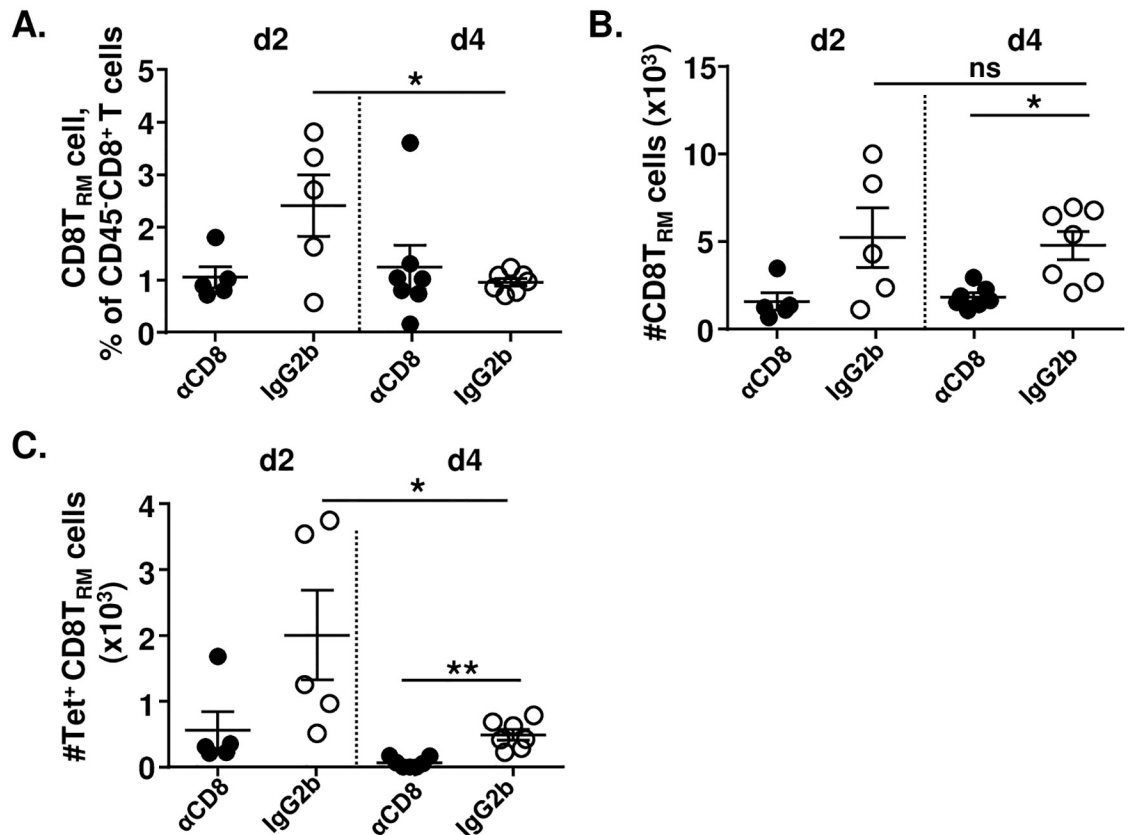
Fig 7. CD8T$_{RM}$ cells do not expand upon IAV challenge. BALB/c mice were immunized with 2×10^5 PFU MCMV^{IVL} via the i.n. route. During latency ($>$ 3 months p.i), mice were i.n. treated with αCD8 (black circle) or IgG2b (white circle) antibodies and challenged with IAV (PR8) (i.n., 1100 FFU) one day after. Anti-CD45 antibodies were injected intravenously 3–5 min before mice euthanasia. Leukocytes were isolated from lung tissue to analyze the CD8$^+$ T cell response on day 2 and day 4 post-challenge. CD8T$_{RM}$ cells were gated within the CD45$^-$unlabeled population. (A) Percentage of CD8T$_{RM}$ cells among CD45$^-$ CD8$^+$ T cell. (B) Counts of CD8T$_{RM}$ cells in the lungs. (C) Counts of IVL-specific CD8T$_{RM}$ cells in the lungs. Two independent experiments were performed and pooled data are shown. Each symbol represents one mouse, n = 5–7. Group means +/- SEM are shown. Significance was assessed by One-way ANOVA test. *P $<$0.05, **P $<$0.01, ns: no significant difference.

https://doi.org/10.1371/journal.ppat.1008036.g007

We show here that robust CD8$^+$ T cell responses against a single MHC-I restricted epitope derived from the HA protein of IAV, promote the clearance of IAV from lungs, but only upon i.n. immunization. While some pathology was observed even in immunized mice, arguing that the protection was not complete, depletion assays confirmed that CD8$^+$ T cells are crucial for the immune protection observed in our model. *Morabito et al.* showed that the volume of MCMV inoculum affects the magnitude of T cell responses [29]. Hence, a larger inoculum volume could have resulted in even stronger lung CD8$^+$ T cell responses and protection. Remarkably, immunization with the same virus dose by the i.p. route induced even higher magnitude of CD8$^+$ T cell responses, but conferred poor protection.

This conundrum was resolved once we noticed that only i.n. immunization induces T$_{RM}$ responses in the lung. CD8T$_{RM}$ cells act as sentinels in the host and form the first line of defense, providing rapid and effective protection to fight against pathogens invasion [27, 29, 31, 45]. Prior studies have revealed that direct delivery of vaccines to the target tissue is necessary for the generation of T$_{RM}$ cells [29, 46] and that sustained lung CD8T$_{RM}$ responses in MCMV-infected mice are generated by immunoproteasome-independent antigenic stimulation [47], akin to the CD8 expansions in memory inflation [21], arguing that their induction

may share similar or overlapping mechanisms. Some prior studies have claimed that skin-resident CD8T$_{RM}$ cells may confer protection in an antigen-unspecific manner [48], whereas others argued that only the antigen-specific CD8T$_{RM}$ cells respond to cognate antigens [49]. MCMV^{WT} induced robust CD8T$_{RM}$ responses in our model, but these were not specific for IAV, and did not provide any protection against IAV in our study. Site-specific anti-CD8α antibody administration depleted CD8T$_{RM}$, and increased IAV titers in immunized mice, indicating that CD8T$_{RM}$ cells facilitated IAV elimination. Thus, the protection against IAV challenge requires antigen-specific CD8T$_{RM}$ cells in our model. However, the weight loss was not different in the early days upon challenge and T$_{RM}$ depletion affected chemokine expression and T cell influx at later time points.

Former studies have described that the inflationary MCMV-specific CD8^{+} T cells induced by intraperitoneal infection display an effector phenotype (KLRG1^{+}CD62L^{-}CD127^{-}) [50, 51]. Mucosal immunization of MCMV^{IVL} affects not only the magnitude but also the quality of CD8^{+} T cells skewing cells towards an effector memory phenotype. Since KLRG1 is assumed a marker for terminally differentiated cells which usually are short-lived [52], the low expression of KLRG1 may contribute to a longer life-span of these cells. Additionally, recent work has demonstrated that KLRG1^{-} CD8^{+} T$_{EM}$ cells traffic and migrate more rapidly to non-lymphoid tissues than the KLRG1^{+} CD8^{+} T$_{EFF}$ cells, which mostly remain in the circulation [53, 54]. Accordingly, this may give us a clue that CD8T$_{EM}$ cells induced by mucosal immunization may rapidly migrate to the lungs and exert immune functionality there. Nonetheless, further studies need to be done to prove this hypothesis.

It has been assumed that CD8T$_{RM}$ cells have poor proliferative capacity upon challenge. Previous work has demonstrated that airway CD8^{+} T cells fail to expand *in vivo* upon intratracheal transfer [36] and that CD8T$_{RM}$ cells induced by MCMV infection display a limited proliferative capacity in salivary glands [55]. However, this is in contrast to two recent studies demonstrating that CD8T$_{RM}$ cells in the skin [49] and FRT [56] maintain the capacity of *in situ* proliferation upon cognate antigen stimulation. Such stimulation differentiates circulating effector memory CD8^{+} T cells into CD8T$_{RM}$ cells without displacing the pre-existing CD8T$_{RM}$ population [49]. In our study, CD8^{+} T cells accumulated in the lungs upon IAV challenge, but the CD8T$_{RM}$ population did not expand and the number of antigen-specific CD8T$_{RM}$ cells even displayed a reduction trend. This appears unrelated to apoptosis, because CD8T$_{RM}$ cells showed less caspase3 expression than circulating CD8^{+} T cells upon challenge. It is possible that CD8T$_{RM}$ cells downregulated CD103 from the cell surface upon activation, and this intriguing question needs to be addressed in future studies. Therefore, our data argued that either lung CD8T$_{RM}$ in general or CD8T$_{RM}$ induced by MCMV i.n. immunization in particular, may behave differently from CD8T$_{RM}$ in other organs. This distinction, however, goes beyond the scope of our current work and remains to be addressed in future studies.

Early upon IAV challenge, not only the IVL-specific CD8^{+} T cells but also the bystander CD8^{+} T cells in the lung tissue increased significantly, indicating that the accumulation was not due to *in situ* proliferation but probably due to recruitment from circulating system. In addition, IAV challenge expanded IVL-specific CD8^{+} T cell counts in the blood and spleen of i.n. immunized mice to levels observed in the i.p. immunized controls, although the levels were significantly lower in the i.n. immunization group before IAV challenge. Overall, these results indicated that i.n. immunization facilitated CD8^{+} T cell responses upon challenge, both locally in the lungs and systemically in the blood and spleen. It is unclear if this apparent alarming function of T$_{RM}$ cells is exclusive to the lung tissue.

We have shown in this study that concentration of CCL3, CCL4 and CXCL9 in the BALF of the MCMV^{IVL} i.n. immunization group is significantly higher than in MCMV^{IVL} i.p. or MCMV^{WT} i.n. immunized mice. Intravital CD45 labeling showed that CD8^{+} T cells

accumulating in the lungs are sequestered from the bloodstream, but not CD8T$_{RM}$, arguing that circulating antigen-specific cells were attracted into the lungs under the presence of mucosa-resident CD8$^+$ T cells. This is in line with the work of *Schenkel* et al. showing a rapid local induction of chemokines CXCL9 and CCL3/4 in the FRT upon re-infection, and recruitment of memory CD8$^+$ T cells from the periphery [28]. Depletion of mucosal CD8$^+$ T cells depressed chemokine levels in the BALF to levels seen in the i.p. immunization group. This, together with the high levels of IFNγ in the MCMV^{IVL} i.n. immunization group and extremely low IFNγ in MCMV^{WT} i.n. immunization points to a putative model where antigen-specific re-stimulation induces IFNγ, which drives chemokine responses that recruit CD8$^+$ T cells from the bloodstream to the lungs. We observed a surprising lower level of IL-6 upon challenge in mice that controlled influenza, because IL-6 is known as a cytokine that is involved in controlling virus infection [57–61]. It is not clear if IL-6 reduction was a consequence of lower virus titers or of negative regulation by T$_{RM}$. *McMaster et al.* showed a reduced IL-6 production accompanied with lower virus titer in the appearance of lung airway CD8T$_{RM}$ cells [36] and this was similar to a report by *Lee et al.* in a clinical study in human patients [62].

In summary, our data demonstrate that CD8T$_{RM}$ cells promote the induction of chemokines, which help to drive the recruitment of IVL-specific CD8$^+$ T cells and facilitates the elimination of IAV. Furthermore, the optimal induction of CD8T$_{RM}$ cells in the lungs by the MCMV vector can be only achieved after i.n. vaccination. Therefore, immunization with an MCMV vector at the local site provided CD8$^+$ T cell-based protection against IAV infection. Our results, therefore, demonstrate that CD8$^+$ T cell induction, and CD8T$_{RM}$ in particular, contribute to vaccination outcomes in influenza infection independently of humoral immune responses, and the selection of the adequate immunization route plays a critical role in terms for promoting superior protective efficacy.

Materials and methods

Ethics statement

Mice were housed and handled in agreement with good animal practice as defined by EU directive EU 2010/63 and ETS 123 and the national animal welfare body "Die Gesellschaft für Versuchstierkunde /Society of Laboratory Animals (GV-SOLAS)". Animal experiments were performed in accordance with the German animal protection law and were approved by the responsible state office (Lower Saxony State Office of Consumer Protection and Food Safety) under permit number: 33.9-42502-04-14/1709.

Mice

BALB/c mice were purchased from Janvier (Le Genest Saint Isle, France) and housed in the animal facility of the HZI Braunschweig under SPF conditions according to FELASA recommendations [63].

Cells

Bone marrow stromal cell line M2-10B4 (CRL-1972) and NIH-3T3 fibroblasts (CRL-1658) were purchased from American Type Culture Collection (ATCC). The cells were maintained in DMEM supplemented with 10% FCS, 1% L-glutamine, and 1% penicillin/streptomycin. C57BL/6 murine embryonic fibroblasts (MEFs) were prepared in-house and maintained as described previously [64].

Viruses

BAC-derived wild-type murine cytomegalovirus (MCMV^{WT} clone: pSM3fr 3.3) [65] was propagated on M2-10B4 lysates and purified on a sucrose cushion as described previously [66]. Virus titers were determined on MEFs by plaque assay as shown elsewhere [67].

Recombinant MCMV was generated by the "en passant mutagenesis", essentially as described previously [68, 69]. In brief, we generated a construct containing an antibiotic resistance cassette coupled with the insertion sequence and the restriction site Sce-I. This construct was flanked by sequences homologous to the target region of insertion within the MCMV BAC genome. Then, the fragment containing the insertion sequences was integrated into the MCMV BAC genome by homologous recombination. In a second step, Sce-I was induced to linearize the BAC followed by a second round of induced homologous recombination to re-circularize it and select for clones that discarded the antibiotic selection marker but retained the inserted sequence.

The PR8M variant of Influenza A/PR/8/34 was obtained from the strain collection at the Institute of Molecular Virology, Muenster, Germany. Virus stocks from chorioallantoic fluid of embryonated chicken eggs were generated as previously described [70].

Tetramers and antibodies

$_{533}$IYSTVASSL$_{541}$ (IVL$_{533-541}$)-tetramer was bought from MBL (cat. NO.TS-M520-1), anti-CD8α depletion antibody (clone: YTS 169.4). Rat IgG2b isotype antibody (clone: LTF-2) was purchased from Bio X Cell. Antibodies for flow cytometry included anti-CD3-APC-eFluor780 (clone: 17A2; eBioscience), anti-CD4-Pacific Blue (clone: GK1.5; BioLegend), anti–CD8α-PerCP/Cy5.5 (clone: 53–6.7; BioLegend), anti-CD11a-PE/Cy7 (clone: 2D7; BD Bioscience), anti–CD44-Alexa Fluor 700 (clone: IM7; BioLegend), anti-CD45-APC-eFluor780 (clone:30-F11;Biolegend), anti-CD62L-eVolve 605 (clone: MEL-14; eBioscience), anti-CD127-PE & PE/Cy7 (clone: A7R34; BioLegend), anti-KLRG1-FITC & BV510 (clone: 2F1/KLRG1; BioLegend), anti-CD103-APC (clone: 2E7; BioLegend), anti-CD69-FITC (clone: H1.2F3; BioLegend) and anti-IFNγ-APC (clone: XMG1.2; BioLegend), anti-Eomes-PE & PE/Cy7 (clone: Dan11mag; eBioscience).

Virus *in vitro* infection

NIH-3T3 cell monolayers were infected with MCMV^{WT} and MCMV^{IVL} at an MOI of 0.1, incubated at 37˚C for 1h, upon which the inoculum was removed, cells were washed with PBS, and supplied with fresh medium. Cells were incubated for 6 days; the supernatant was harvested every day and stored at -80˚C until titration.

Virus *in vivo* infection

6 to 8 weeks old BALB/c female mice were infected with 2×10^5 PFU MCMV^{WT} and MCMV^{IVL} diluted in PBS. For i.p. infection, 100 µl virus dilution was injected. For i.n. infection, mice were first anesthetized with ketamine (10 mg/ml) and xylazine (1 mg/ml) in 0.9% NaCl (100 µl/10 g body weight), then administered with 20 µl of virus suspension onto nostrils [35]. For IAV challenge, BALB/c mice that were latently (> 3 months) immunized with MCMV were i.n. inoculated with 220 focus forming units (FFU) or with 1100 FFU of PR8M influenza virus as described previously [35].

Infectious virus quantification (MCMV)

MCMV virus from organ homogenates was titrated on MEFs with centrifugal enhancement as described previously [17].

Infectious virus quantification (IAV)

Mice were sacrificed by CO_2 inhalation, whole lungs were excised and mechanically homogenized using a tissue homogenizer. Tissue homogenates were spun down and supernatants were stored at -70˚C. Lung virus titers were determined by using the focus-forming assay (FFA), as described before [70] with minor modifications. Briefly, MDCK cells were cultured in MEM, supplemented with 10% FCS, 1% penicillin/streptomycin. Supernatants of lung tissue homogenates were serially diluted in DMEM, supplemented with 0.1% BSA and N-acetylated trypsin (NAT; 2.5 μg/ml) and added to the MDCK cell monolayers. After 1h, cells were overlaid with DMEM supplemented with 1% Avicel, 0.1% BSA and NAT (2.5 μg/ml). After 24h cells were fixed with 4% PFA and incubated with quenching solution (PBS, 0.5% Triton X-100, 20 mM Glycin). Cells were then treated with blocking buffer (PBS, 1% BSA, 0.5% Tween20). Focus forming spots were identified using primary polyclonal goat anti-H1N1 IgG (Virostat), secondary polyclonal rabbit anti-goat IgG conjugated with horseradish peroxidase (KPL) and TrueBlue™ peroxidase substrate (KPL). Viral titers were calculated as FFU per ml of lung tissue homogenate.

Isolation of lymphocytes from blood and organs

Blood, spleen and mLNs were prepared as described previously [35]. Lungs were perfused by injecting 5–10 ml PBS into the right heart ventricle. The lungs were cut into small pieces, resuspended in 1 ml RPMI1640 (0.5% FCS), and digested with 1 ml of RPMI1640 with DNase I (Sigma-Aldrich Chemie) and Collagenase I (ROCKLAND™) in a shaker at 37˚C for 30 min. Digested tissue was passed through cell strainers and single cell suspensions were washed with RPMI1640, centrifuged at 500x g for 10 min. Subsequently, the cells were resuspended in 7 ml of 40% Easycoll solution (Biochrom), overlayed onto 6 ml of 70% Easycoll solution in a 15 ml Falcon and centrifuged at 25 min at 1000x g at room temperature. The interface layer was transferred to a 5 ml tube, washed, and resuspended in RPMI1640 (10% FCS).

Peptide stimulation

T cells were stimulated with peptides (1 μg/ml) in 85 μl RPMI 1640 for 1h at 37˚C, supplemented with brefeldin A (10 μg/ml in 15 μl RPMI 1640) and incubated for additional 5h at 37˚C. Cells incubated without any peptide in the same condition were used as negative controls. Cytokine responses were detected by intracellular cytokine staining.

Cell surface staining, intracellular cytokine staining for flow cytometry

Blood cells and lymphocytes from spleen, lung and mLNs were stained with $IVL_{533-541}$-tetramer-PE and surface antibodies for 30 min, washed with FACS buffer and analyzed. For intracellular cytokine stainings, the cells were first stained with cell surface antibodies for 30 min, washed and fixed with 100 μl IC fixation buffer (eBioscience) for 5 min at 4˚C. Following this, cells were permeabilized for 3 min with 100 μl permeabilization buffer (eBioscience) and incubated with anti-IFNγ antibody for 30 min. Afterwards, cells were washed with FACS buffer and acquired using an LSR-Fortessa flow cytometer (BD Bioscience).

In vivo cell labeling

Mice were intravenously (i.v.) injected with 3 μg anti-CD45-APC/eFluor780 (clone: 30-F11; BioLegend). Mice were euthanized 3–5 min after injection, and blood, spleen and lungs were collected. Following their isolation from the respective compartment, lymphocytes were stained and analyzed as described above.

In vivo CD8^{+} T cell depletion

For systemic *in vivo* CD8^{+} T cell depletion, published protocols [71, 72] were adopted as follows. BALB/c mice were i.p. injected with 200 μg anti-CD8α (αCD8: clone: YTS 169.4) or isotype antibody (Rat IgG2b: clone: LTF-2; Bio X Cell) one day before IAV challenge. To deplete mucosal CD8^{+} T cells in the lungs, BALB/c mice were i.n. administered 10 μg αCD8 or IgG2b in 20 μl of PBS one day before IAV challenge [40].

Collection of bronchoalveolar lavage fluid (BALF)

Mice were sacrificed by CO_2 inhalation, the chest cavity was opened and skin and muscle around the neck were gently removed to expose the trachea. A catheter was inserted and the lungs were carefully flushed with 1 mL PBS via the trachea. The BALF was transferred into a 1.5 ml tube and stored on ice. The BALF was centrifuged at 500x g at 4˚C for 10 min. The supernatant was aliquoted and stored at -80˚C until further analysis.

Cytokine and chemokine quantification

Mouse IFNγ enzyme-linked immunosorbent assay (ELISA) MAX™ kits (BioLegend) and the bead-based immunoassay LEGENDplex™ Mouse Inflammation Panel (13-plex, BioLegend) were used to quantify IFNγ and other cytokine levels in the BALF according to the manufacturer's instructions. The bead-based immunoassay LEGENDplex Mouse Pro-inflammation Chemokine Panel (13-plex, BioLegend) was used to quantify multiple chemokine levels in the BALF.

Histopathology

Lungs were harvested from BALB/c mice that were latently infected with MCMV[WT] and MCMV[IVL] and challenged with IAV during latency. Lungs were fixed in 4% formalin, paraffin embedded, sliced and hematoxylin and eosin (H&E) stained according to standard laboratory procedures.

Statistics

One-way ANOVA analysis was used to compare multiple groups at single time points. Two-way ANOVA analysis was used to compare different groups at multiple time points. Comparisons between two groups were performed using Mann-Whitney U test (two-tailed). Statistical analysis was performed using GraphPad Prism 7.

Supporting information

S1 Fig. Gating strategy of flow cytometry. BALB/c mice were immunized with 2 x 10^{5} PFU MCMV[IVL] via the i.p. or i.n. route. During latency ($>$ 3 months p.i), Leukocytes from blood, spleen and lungs were stained with cell surface markers CD3, CD4, CD8, CD11a, CD69, CD103, KLRG1, CD62L, IVL-tetramer and analyzed by flow cytometry. For *in vivo* labeling, anti-CD45 antibodies were injected intravenously 3–5 min before mice euthanasia. Gating

strategy of each cell subset is shown.
(TIF)

S2 Fig. Efficiency of *in vivo* CD8$^+$ T cell depletion. BALB/c mice were immunized with 2 x 10^5 PFU MCMV^{IVL} by the i.n. route. (A) During latency ($>$ 3 months p.i), mice were injected 200 µg αCD8 antibody (i.p.) to deplete total CD8$^+$ T cells. Same amount of IgG2b antibody was given as isotype control. Leukocytes from blood, spleen and lungs were analyzed by flow cytometry and representative flow cytometric panels in blood, spleen and lungs on day 1 post-depletion are shown. (B-C) Mice were administered with 10 µg αCD8 antibody (i.n.) to deplete airway CD8$^+$ T cells in the lungs or IgG2b as a control. (B) The number of IVL-tetramer$^+$ CD8T$_{RM}$ cells and circulating CD8$^+$ T cells (CD45$^+$) in the lungs on day 1 post airway CD8$^+$ T cell depletion. (C) The number of IVL-specific and total CD8$^+$ T cells in the peripheral blood on day 1 post airway CD8$^+$ T cell depletion. Bars indicate means, error bars are SEM.
(TIF)

S3 Fig. MCMV^{WT} mucosal immunization induces IVL-unspecific CD8T$_{RM}$ and CD8T$_{RM}$ cells express low Eomes and caspase3/7. BALB/c mice were immunized with 2 x 10^5 PFU MCMV^{WT} via the i.n. route. During latency ($>$ 3 months p.i), leukocytes were isolated from lungs, stained with cell surface markers against CD4, CD8, CD69, CD103 before flow cytometry. (A) Representative dot plots of CD8T$_{RM}$ and IVL-specific CD8T$_{RM}$ cells. (B, C) BALB/c mice were immunized with 2 x 10^5 PFU MCMV^{IVL} via the i.n. or i.p. route. (B) Percentage of CD69$^+$CD103$^-$CD8$^+$ T cells in the lungs. (C) The number of CD69$^+$CD103$^-$CD8$^+$ T cells in the lungs. (D) Eomes expression on different subsets of CD8$^+$ T cells in the lungs. (E) Percentage of caspase3/7$^+$ cells among CD8T$_{RM}$ and circulating CD8$^+$ T (CD45$^+$) cells. (F) Percentage of caspase3/7$^+$ cells among tetramer$^+$ CD8T$_{RM}$ and circulating CD8$^+$ T (CD45$^+$) cells. Two independent experiments were performed and pooled data are shown. Each symbol represents one mouse, n = 5–9. Group means +/- SEM are shown. Significance was assessed by Mann-Whitney U test. **P $<$0.01, ***P $<$0.001, ns: no significance.
(TIF)

S4 Fig. The phenotype of IVL-specific CD8$^+$ T cells. BALB/c mice were immunized with 2 x 10^5 PFU MCMV^{IVL} via the i.p. or i.n. route. During latency ($>$ 3 months p.i), anti-CD45 antibodies were injected intravenously 3–5 min before mice euthanasia. Leukocytes from blood, spleen and lungs were stained with cell surface markers CD3, CD4, CD8, CD11a, KLRG1, CD62L, IVL-tetramer and analyzed by flow cytometry. T$_{EFF}$ cells are defined as KLRG1$^+$CD62L$^-$, T$_{EM}$ as KLRG1$^-$CD62L$^-$and T$_{CM}$ as KLRG1$^-$CD62L$^+$. (A) The percentages of each phenotype subset among CD45$^-$ tetramer$^+$ CD8$^+$ T cells in the lungs and spleen. (B) The percentages of each phenotype subset among CD45$^+$ tetramer$^+$ CD8$^+$ T cells and tetramer$^+$ CD8T$_{RM}$ cells in the lungs, spleen and blood. (C) The percentages of each phenotype subset among tetramer$^+$ CD8T$_{RM}$ cells in the lungs. Two independent experiments were performed and pooled data are shown, n = 5. Each symbol represents one mouse. Group means +/- SEM are shown. Significance was assessed by One-way ANOVA and Two-way ANOVA test. ****P $<$0.0001.
(TIF)

S5 Fig. Inflammatory cytokines in the BALF upon IAV challenge. BALB/c mice were immunized with 2 x 10^5 PFU MCMV^{IVL} via the i.n. or i.p. route or with MCMV^{WT} via the i.n. route. During latency ($>$ 3 months p.i), MCMV^{IVL} (i.n.) immunized mice were administered with 10 µg αCD8 or 10 µg IgG2b antibody (i.n.). MCMV^{IVL} (i.p.) and MCMV^{WT} (i.n.) immunized mice were administered with 10 µg IgG2b antibody (i.n.). One day later, animals were challenged with IAV (PR8) (i.n., 1100 FFU). On day 2 and day 4 post-challenge, BALF was

harvested and measured cytokines production by bio-plexing. The concentration of (A) IFNγ and (B) IL-6 in the BALF on day 4 post-challenge. Two independent experiments were performed and pooled data are shown. Each symbol represents one mouse, n = 5–7. Group means +/- SEM are shown. (C) Cytokine concentrations in the BALF in different immunization group on day 2 and day 4 post-challenge. Bars indicate means, error bars are SEM. Two independent experiments were performed and pooled data are shown. Each symbol represents one mouse, n = 5–7. Significance was assessed by One-way ANOVA test. *P <0.05, ***P <0.001.
(TIF)

S6 Fig. Mucosal immunization with MCMV^{IVL} induced vigorous CD8⁺ T cell responses in blood, spleen and lungs. BALB/c mice were immunized with 2 x 10^5 PFU MCMV[IVL] by the i.n. or i.p. route or with MCMV[WT] by the i.n. route. During latency (> 3 months p.i), mice were challenged with IAV (PR8) (i.n., 1100 FFU) one day after airway CD8^{+} T cell depletion. On day 4 post-challenge, anti-CD45 antibodies were injected intravenously 3–5 min before mice euthanasia. Leukocytes were isolated from lung, BAL, blood and spleen. (A-B) Count of IVL-specific CD8^{+} T cells in the lungs (A) and BAL (B). (C-D) Percentage of IVL-specific CD8^{+} T cells among CD8^{+} T cells in the blood (C) and spleen (D). (E-F) Count of IVL-specific CD8^{+} T cell in the blood (E) and spleen (F). Two independent experiments were performed and pooled data are shown. Each symbol represents one mouse, n = 5–7. Group means +/- SEM are shown. Significance was assessed by One-way ANOVA test. *P <0.05, **P <0.01.
(TIF)

S7 Fig. Airway CD8⁺ T cell depletion does not affect CD4⁺ T cells upon IAV challenge. BALB/c mice were immunized with 2 x 10^5 PFU MCMV[IVL] by the i.n. route. During latency (> 3 months p.i), mice were challenged with IAV (PR8) (i.n., 1100 FFU) one day after airway CD8^{+} T cell depletion. On day 2 and day 4 post-challenge, anti-CD45 antibodies were injected intravenously 3–5 min before mice euthanasia. Leukocytes were isolated from lungs and BAL. CD4^{+} T cell numbers in the lungs are shown. (A) The number of total CD4^{+} T cells. (B) The number of CD45^{-} CD4^{+} T cells. (C) The number of CD4^{+} T cells in the BAL. Two independent experiments were performed and pooled data are shown. Each symbol represents one mouse, n = 5–7. Group means +/- SEM are shown.
(TIF)

Acknowledgments

Author Contributions

Conceptualization: Luka Čičin-Šain.

Data curation: Xiaoyan Zheng, Jennifer D. Oduro, Julia D. Boehme, Lisa Borkner, Thomas Ebensen, Ulrike Heise, Marcus Gereke, Marina C. Pils, Dunja Bruder, Luka Čičin-Šain.

Formal analysis: Xiaoyan Zheng, Lisa Borkner, Ulrike Heise, Dunja Bruder, Luka Čičin-Šain.

Funding acquisition: Luka Čičin-Šain.

Investigation: Xiaoyan Zheng, Jennifer D. Oduro, Julia D. Boehme, Lisa Borkner, Thomas Ebensen, Marcus Gereke.

Methodology: Julia D. Boehme, Astrid Krmpotic, Carlos A. Guzmán, Luka Čičin-Šain.

Project administration: Luka Čičin-Šain.

Resources: Astrid Krmpotic.

Supervision: Marina C. Pils, Carlos A. Guzmán, Dunja Bruder, Luka Čičin-Šain.

Validation: Lisa Borkner.

Writing – original draft: Xiaoyan Zheng.

Writing – review & editing: Astrid Krmpotic, Carlos A. Guzmán, Dunja Bruder, Luka Čičin-Šain.

References

1. WHO. Influenza (Seasonal) Fact sheet N˚211". who.int. 2014; http://www.who.int/en/news-room/fact-sheets/detail/influenza-(seasonal).

2. Barria M.I., et al., Localized mucosal response to intranasal live attenuated influenza vaccine in adults. J Infect Dis, 2013. 207(1): p. 115–24. https://doi.org/10.1093/infdis/jis641 PMID: 23087433

3. Ilyushina N.A., et al., Live attenuated and inactivated influenza vaccines in children. J Infect Dis, 2015. 211(3): p. 352–60. https://doi.org/10.1093/infdis/jiu458 PMID: 25165161

4. Eichelberger M., et al., Clearance of influenza virus respiratory infection in mice lacking class I major histocompatibility complex-restricted CD8+ T cells. J Exp Med, 1991. 174(4): p. 875–80. https://doi.org/10.1084/jem.174.4.875 PMID: 1919440

5. Bender B.S., et al., Transgenic mice lacking class I major histocompatibility complex-restricted T cells have delayed viral clearance and increased mortality after influenza virus challenge. J Exp Med, 1992. 175(4): p. 1143–5. https://doi.org/10.1084/jem.175.4.1143 PMID: 1552285

6. Yager E.J., et al., Age-associated decline in T cell repertoire diversity leads to holes in the repertoire and impaired immunity to influenza virus. J Exp Med, 2008. 205(3): p. 711–23. https://doi.org/10.1084/jem.20071140 PMID: 18332179

7. Baumgarth N. and Kelso A., In vivo blockade of gamma interferon affects the influenza virus-induced humoral and the local cellular immune response in lung tissue. J Virol, 1996. 70(7): p. 4411–8. PMID: 8676464

8. Topham D.J., Tripp R.A., and Doherty P.C., CD8+ T cells clear influenza virus by perforin or Fas-dependent processes. J Immunol, 1997. 159(11): p. 5197–200. PMID: 9548456

9. Sylwester A.W., et al., Broadly targeted human cytomegalovirus-specific CD4+ and CD8+ T cells dominate the memory compartments of exposed subjects. J Exp Med, 2005. 202(5): p. 673–85. https://doi.org/10.1084/jem.20050882 PMID: 16147978

10. Holtappels R., et al., Enrichment of immediate-early 1 (m123/pp89) peptide-specific CD8 T cells in a pulmonary CD62L(lo) memory-effector cell pool during latent murine cytomegalovirus infection of the lungs. J Virol, 2000. 74(24): p. 11495–503. https://doi.org/10.1128/jvi.74.24.11495-11503.2000 PMID: 11090146

11. Karrer U., et al., Memory inflation: continuous accumulation of antiviral CD8+ T cells over time. J Immunol, 2003. 170(4): p. 2022–9. https://doi.org/10.4049/jimmunol.170.4.2022 PMID: 12574372

12. Munks M.W., et al., Four distinct patterns of memory CD8 T cell responses to chronic murine cytomegalovirus infection. J Immunol, 2006. 177(1): p. 450–8. https://doi.org/10.4049/jimmunol.177.1.450 PMID: 16785542

13. Podlech J., et al., Murine model of interstitial cytomegalovirus pneumonia in syngeneic bone marrow transplantation: persistence of protective pulmonary CD8-T-cell infiltrates after clearance of acute infection. J Virol, 2000. 74(16): p. 7496–507. https://doi.org/10.1128/jvi.74.16.7496-7507.2000 PMID: 10906203

14. Karrer U., et al., Expansion of protective CD8+ T-cell responses driven by recombinant cytomegaloviruses. J Virol, 2004. 78(5): p. 2255–64. https://doi.org/10.1128/JVI.78.5.2255-2264.2004 PMID: 14963122

15. Tsuda Y., et al., A replicating cytomegalovirus-based vaccine encoding a single Ebola virus nucleoprotein CTL epitope confers protection against Ebola virus. PLoS Negl Trop Dis, 2011. 5(8): p. e1275. https://doi.org/10.1371/journal.pntd.0001275 PMID: 21858240

16. Hansen S.G., et al., Profound early control of highly pathogenic SIV by an effector memory T-cell vaccine. Nature, 2011. 473(7348): p. 523–7. https://doi.org/10.1038/nature10003 PMID: 21562493

17. Dekhtiarenko I., et al., The context of gene expression defines the immunodominance hierarchy of cytomegalovirus antigens. J Immunol, 2013. 190(7): p. 3399–409. https://doi.org/10.4049/jimmunol.1203173 PMID: 23460738

18. Borkner L., et al., Immune Protection by a Cytomegalovirus Vaccine Vector Expressing a Single Low-Avidity Epitope. J Immunol, 2017. 199(5): p. 1737–1747. https://doi.org/10.4049/jimmunol.1602115 PMID: 28768725

19. Beverley P.C., et al., A novel murine cytomegalovirus vaccine vector protects against Mycobacterium tuberculosis. J Immunol, 2014. 193(5): p. 2306–16. https://doi.org/10.4049/jimmunol.1302523 PMID: 25070842

20. Klyushnenkova E.N., et al., A cytomegalovirus-based vaccine expressing a single tumor-specific CD8+ T-cell epitope delays tumor growth in a murine model of prostate cancer. J Immunother, 2012. 35(5): p. 390–9. https://doi.org/10.1097/CJI.0b013e3182585d50 PMID: 22576344

21. Dekhtiarenko I., et al., Peptide Processing Is Critical for T-Cell Memory Inflation and May Be Optimized to Improve Immune Protection by CMV-Based Vaccine Vectors. PLoS Pathog, 2016. 12(12): p. e1006072. https://doi.org/10.1371/journal.ppat.1006072 PMID: 27977791

22. Marzi A., et al., Cytomegalovirus-based vaccine expressing Ebola virus glycoprotein protects nonhuman primates from Ebola virus infection. Sci Rep, 2016. 6: p. 21674. https://doi.org/10.1038/srep21674 PMID: 26876974

23. Hansen S.G., et al., Cytomegalovirus vectors violate CD8+ T cell epitope recognition paradigms. Science, 2013. 340(6135): p. 1237874. https://doi.org/10.1126/science.1237874 PMID: 23704576

24. Erkes D.A., Wilski N.A., and Snyder C.M., Intratumoral infection by CMV may change the tumor environment by directly interacting with tumor-associated macrophages to promote cancer immunity. Hum Vaccin Immunother, 2017. 13(8): p. 1778–1785. https://doi.org/10.1080/21645515.2017.1331795 PMID: 28604162

25. Qiu Z., et al., Cytomegalovirus-Based Vaccine Expressing a Modified Tumor Antigen Induces Potent Tumor-Specific CD8(+) T-cell Response and Protects Mice from Melanoma. Cancer Immunol Res, 2015. 3(5): p. 536–46. https://doi.org/10.1158/2326-6066.CIR-14-0044 PMID: 25633711

26. Gebhardt T., et al., Memory T cells in nonlymphoid tissue that provide enhanced local immunity during infection with herpes simplex virus. Nat Immunol, 2009. 10(5): p. 524–30. https://doi.org/10.1038/ni.1718 PMID: 19305395

27. Wakim L.M., et al., The molecular signature of tissue resident memory CD8 T cells isolated from the brain. J Immunol, 2012. 189(7): p. 3462–71. https://doi.org/10.4049/jimmunol.1201305 PMID: 22922816

28. Schenkel J.M., et al., Sensing and alarm function of resident memory CD8(+) T cells. Nat Immunol, 2013. 14(5): p. 509–13. https://doi.org/10.1038/ni.2568 PMID: 23542740

29. Morabito K.M., et al., Intranasal administration of RSV antigen-expressing MCMV elicits robust tissue-resident effector and effector memory CD8+ T cells in the lung. Mucosal Immunol, 2017. 10(2): p. 545–554. https://doi.org/10.1038/mi.2016.48 PMID: 27220815

30. Mackay L.K., et al., The developmental pathway for CD103(+)CD8+ tissue-resident memory T cells of skin. Nat Immunol, 2013. 14(12): p. 1294–301. https://doi.org/10.1038/ni.2744 PMID: 24162776

31. Jiang X., et al., Skin infection generates non-migratory memory CD8+ T(RM) cells providing global skin immunity. Nature, 2012. 483(7388): p. 227–31. https://doi.org/10.1038/nature10851 PMID: 22388819

32. Lapuente D., et al., IL-1beta as mucosal vaccine adjuvant: the specific induction of tissue-resident memory T cells improves the heterosubtypic immunity against influenza A viruses. Mucosal Immunol, 2018. 11(4): p. 1265–1278. https://doi.org/10.1038/s41385-018-0017-4 PMID: 29545648

33. Smith C.J., et al., Murine CMV Infection Induces the Continuous Production of Mucosal Resident T Cells. Cell Rep, 2015. 13(6): p. 1137–1148. https://doi.org/10.1016/j.celrep.2015.09.076 PMID: 26526996

34. Baumann N.S., et al., Tissue maintenance of CMV-specific inflationary memory T cells by IL-15. PLoS Pathog, 2018. 14(4): p. e1006993. https://doi.org/10.1371/journal.ppat.1006993 PMID: 29652930

35. Oduro J.D., et al., Murine cytomegalovirus (CMV) infection via the intranasal route offers a robust model of immunity upon mucosal CMV infection. J Gen Virol, 2016. 97(1): p. 185–95. https://doi.org/10.1099/jgv.0.000339 PMID: 26555192

36. McMaster S.R., et al., Airway-Resident Memory CD8 T Cells Provide Antigen-Specific Protection against Respiratory Virus Challenge through Rapid IFN-gamma Production. J Immunol, 2015. 195(1): p. 203–9. https://doi.org/10.4049/jimmunol.1402975 PMID: 26026054

37. Hombrink P., et al., Programs for the persistence, vigilance and control of human CD8+ lung-resident memory T cells. Nat Immunol, 2016. 17(12): p. 1467–1478. https://doi.org/10.1038/ni.3589 PMID: 27776108

38. Tamura M., et al., Definition of amino acid residues on the epitope responsible for recognition by influenza A virus H1-specific, H2-specific, and H1- and H2-cross-reactive murine cytotoxic T-lymphocyte clones. J Virol, 1998. 72(11): p. 9404–6. PMID: 9765498

39. Flynn K.J., et al., Virus-specific CD8+ T cells in primary and secondary influenza pneumonia. Immunity, 1998. 8(6): p. 683–91. PMID: 9655482

40. Slutter B., et al., Lung airway-surveilling CXCR3(hi) memory CD8(+) T cells are critical for protection against influenza A virus. Immunity, 2013. 39(5): p. 939–48. https://doi.org/10.1016/j.immuni.2013.09.013 PMID: 24238342

41. Samuel C.E., Antiviral actions of interferon. Interferon-regulated cellular proteins and their surprisingly selective antiviral activities. Virology, 1991. 183(1): p. 1–11. https://doi.org/10.1016/0042-6822(91)90112-o PMID: 1711253

42. Cheuk S., et al., CD49a Expression Defines Tissue-Resident CD8(+) T Cells Poised for Cytotoxic Function in Human Skin. Immunity, 2017. 46(2): p. 287–300. https://doi.org/10.1016/j.immuni.2017.01.009 PMID: 28214226

43. Topham D.J. and Reilly E.C., Tissue-Resident Memory CD8(+) T Cells: From Phenotype to Function. Front Immunol, 2018. 9: p. 515. https://doi.org/10.3389/fimmu.2018.00515 PMID: 29632527

44. Wells M.A., Albrecht P., and Ennis F.A., Recovery from a viral respiratory infection. I. Influenza pneumonia in normal and T-deficient mice. J Immunol, 1981. 126(3): p. 1036–41. PMID: 6970211

45. Pizzolla A., et al., Resident memory CD8+ T cells in the upper respiratory tract prevent pulmonary influenza virus infection. Sci Immunol, 2017. 2(12).

46. Zens K.D., Chen J.K., and Farber D.L., Vaccine-generated lung tissue-resident memory T cells provide heterosubtypic protection to influenza infection. JCI Insight, 2016. 1(10).

47. Morabito K.M., et al., Memory Inflation Drives Tissue-Resident Memory CD8(+) T Cell Maintenance in the Lung After Intranasal Vaccination With Murine Cytomegalovirus. Front Immunol, 2018. 9: p. 1861. https://doi.org/10.3389/fimmu.2018.01861 PMID: 30154789

48. Ariotti S., et al., T cell memory. Skin-resident memory CD8(+) T cells trigger a state of tissue-wide pathogen alert. Science, 2014. 346(6205): p. 101–5. https://doi.org/10.1126/science.1254803 PMID: 25278612

49. Park S.L., et al., Local proliferation maintains a stable pool of tissue-resident memory T cells after antiviral recall responses. Nat Immunol, 2018. 19(2): p. 183–191. https://doi.org/10.1038/s41590-017-0027-5 PMID: 29311695

50. Sierro S., Rothkopf R., and Klenerman P., Evolution of diverse antiviral CD8+ T cell populations after murine cytomegalovirus infection. Eur J Immunol, 2005. 35(4): p. 1113–23. https://doi.org/10.1002/eji.200425534 PMID: 15756645

51. Snyder C.M., et al., Memory inflation during chronic viral infection is maintained by continuous production of short-lived, functional T cells. Immunity, 2008. 29(4): p. 650–9. https://doi.org/10.1016/j.immuni.2008.07.017 PMID: 18957267

52. Henson S.M. and Akbar A.N., KLRG1—more than a marker for T cell senescence. Age (Dordr), 2009. 31(4): p. 285–91.

53. Osborn J.F., et al., Enzymatic synthesis of core 2 O-glycans governs the tissue-trafficking potential of memory CD8(+) T cells. Sci Immunol, 2017. 2(16).

54. Gerlach C., et al., The Chemokine Receptor CX3CR1 Defines Three Antigen-Experienced CD8 T Cell Subsets with Distinct Roles in Immune Surveillance and Homeostasis. Immunity, 2016. 45(6): p. 1270–1284. https://doi.org/10.1016/j.immuni.2016.10.018 PMID: 27939671

55. Thom J.T., et al., The Salivary Gland Acts as a Sink for Tissue-Resident Memory CD8(+) T Cells, Facilitating Protection from Local Cytomegalovirus Infection. Cell Rep, 2015. 13(6): p. 1125–36. https://doi.org/10.1016/j.celrep.2015.09.082 PMID: 26526997

56. Beura L.K., et al., Intravital mucosal imaging of CD8(+) resident memory T cells shows tissue-autonomous recall responses that amplify secondary memory. Nat Immunol, 2018. 19(2): p. 173–182. https://doi.org/10.1038/s41590-017-0029-3 PMID: 29311694

57. Yoshizaki K., et al., Interleukin 6 and expression of its receptor on epidermal keratinocytes. Cytokine, 1990. 2(5): p. 381–7. PMID: 2129417

58. Scheller J., et al., The pro- and anti-inflammatory properties of the cytokine interleukin-6. Biochim Biophys Acta, 2011. 1813(5): p. 878–88. https://doi.org/10.1016/j.bbamcr.2011.01.034 PMID: 21296109

59. Murphy E.A., et al., Effect of IL-6 deficiency on susceptibility to HSV-1 respiratory infection and intrinsic macrophage antiviral resistance. J Interferon Cytokine Res, 2008. 28(10): p. 589–95. https://doi.org/10.1089/jir.2007.0103 PMID: 18778200

60. Strestik B.D., et al., The role of IL-5, IL-6 and IL-10 in primary and vaccine-primed immune responses to infection with Friend retrovirus (Murine leukaemia virus). J Gen Virol, 2001. 82(Pt 6): p. 1349–54. https://doi.org/10.1099/0022-1317-82-6-1349 PMID: 11369878

61. Harker J.A., et al., Late interleukin-6 escalates T follicular helper cell responses and controls a chronic viral infection. Science, 2011. 334(6057): p. 825–9. https://doi.org/10.1126/science.1208421 PMID: 21960530

62. Lee N., et al., Hypercytokinemia and hyperactivation of phospho-p38 mitogen-activated protein kinase in severe human influenza A virus infection. Clin Infect Dis, 2007. 45(6): p. 723–31. https://doi.org/10.1086/520981 PMID: 17712756

63. Mahler Convenor M., et al., FELASA recommendations for the health monitoring of mouse, rat, hamster, guinea pig and rabbit colonies in breeding and experimental units. Lab Anim, 2014. 48(3): p. 178–192. https://doi.org/10.1177/0023677213516312 PMID: 24496575

64. Reddehase M.J., Podlech J., and Grzimek N.K., Mouse models of cytomegalovirus latency: overview. J Clin Virol, 2002. 25 Suppl 2: p. S23–36.

65. Jordan S., et al., Virus progeny of murine cytomegalovirus bacterial artificial chromosome pSM3fr show reduced growth in salivary Glands due to a fixed mutation of MCK-2. J Virol, 2011. 85(19): p. 10346–53. https://doi.org/10.1128/JVI.00545-11 PMID: 21813614

66. Dag F., et al., Reversible silencing of cytomegalovirus genomes by type I interferon governs virus latency. PLoS Pathog, 2014. 10(2): p. e1003962. https://doi.org/10.1371/journal.ppat.1003962 PMID: 24586165

67. Cicin-Sain L., Podlech J., Messerle M., Reddehase M. J., and Koszinowski U. H., Frequent coinfection of cells explains functional in vivo complementation between cytomegalovirus variants in the multiply infected host. Journal of Virology, 2005. 79: p. 9492–9502. https://doi.org/10.1128/JVI.79.15.9492-9502.2005 PMID: 16014912

68. Tischer B.K., Smith G.A., and Osterrieder N., En passant mutagenesis: a two step markerless red recombination system. Methods Mol Biol, 2010. 634: p. 421–30. https://doi.org/10.1007/978-1-60761-652-8_30 PMID: 20677001

69. Dekhtiarenko I., Cicin-Sain L., and Messerle M., Use of recombinant approaches to construct human cytomegalovirus mutants. Methods Mol Biol, 2014. 1119: p. 59–79. https://doi.org/10.1007/978-1-62703-788-4_5 PMID: 24639218

70. Blazejewska P., et al., Pathogenicity of different PR8 influenza A virus variants in mice is determined by both viral and host factors. Virology, 2011. 412(1): p. 36–45. https://doi.org/10.1016/j.virol.2010.12.047 PMID: 21256531

71. Salem M.L. and Hossain M.S., In vivo acute depletion of CD8(+) T cells before murine cytomegalovirus infection upregulated innate antiviral activity of natural killer cells. Int J Immunopharmacol, 2000. 22(9): p. 707–18. https://doi.org/10.1016/s0192-0561(00)00033-3 PMID: 10884591

72. Kruisbeek A.M., In vivo depletion of CD4- and CD8-specific T cells. Curr Protoc Immunol, 2001. Chapter 4: p. Unit 4 1.